# Radiative Decays

Chris Sachrajda
University of Southampton

*Isospin -Breaking Effects on Precision Observable in Lattice QCD*
*MITP - Mainz - 26th July 2024*

University of Southampton

# Outline of Talk

1. Introductory Remarks

2. $P \to \ell \nu_\ell \gamma$ Radiative Decays

3. $\bar{B}_s \to \mu^+ \mu^- \gamma$ at large $q^2$

    - Contributions which we are able to compete precisely
      $$(\mathbf{F}_\mathbf{V},\ F_A,\ F_{TV},\ F_{TA})$$
    - Contributions which we can only calculate approximately, but adequately $(\bar{F}_T)$
    - Contributions which we are not yet able to compute on the lattice, but are striving to do so (charming penguins)

4. $P \to \ell \nu_\ell\ \ell'^+ \ell'^-$ Radiative Decays

# 1. Introduction

- Our computations of radiative decays started with our major study of QED corrections to leptonic decays of pseudoscalar mesons.

QED Corrections to Hadronic Processes in Lattice QCD,
N.Carrasco, V.Lubicz, G.Martinelli, CTS, N.Tantalo, C.Tarantino and M.Testa, arXiv:1502.00257

$$\Gamma(\Delta E_\gamma) = \Gamma_0(P \to \ell \bar{\nu}_\ell) + \Gamma_1(P \to \ell \bar{\nu}_\ell \gamma) = \Gamma_0 + \int_0^{2\Delta E_\gamma / m_P} dx_\gamma \, \frac{d\Gamma_1}{dx_\gamma} \qquad \left(x_\gamma = \frac{2E_\gamma}{m_P}\right)$$

$$= \lim_{L\to\infty} \left[\Gamma_0(L) - \Gamma_0^{\rm pt}(\mu_\gamma, L)\right] + \lim_{\mu_\gamma \to 0} \left[\Gamma_0^{\rm pt}(\mu_\gamma) + \Gamma_1^{\rm pt}(\Delta E_\gamma, \mu_\gamma)\right] + \Gamma_1^{\rm SD}(\Delta E_\gamma) + \Gamma_1^{\rm INT}(\Delta E_\gamma)$$

  - pt = ”pointlike”, SD = ”Structure Dependent”, INT = ”Interference”

- Initially we suggested $\Delta E_\gamma$ to be small ( $\simeq 20\,\mathrm{MeV}$) so that $\Gamma_1^{\rm SD}$ and $\Gamma_1^{\rm INT}$ can be neglected.
  - Applicable for kaons and pions.

- Subsequently we have been computing $\Gamma_1$ for larger values of $\Delta E_\gamma$ , including the SD and INT contributions.

First lattice calculation of radiative leptonic decay rates of pseudoscalar mesons, A.Desiderio et al., arXiv:2006.05358

  - This allows the evaluation of $O(\alpha_{\rm em})$ corrections to leptonic decays for all stable pseudoscalar mesons.

# 2. $\mathrm{P} \to \ell\nu_\ell\gamma$ radiative decays - the form factors.

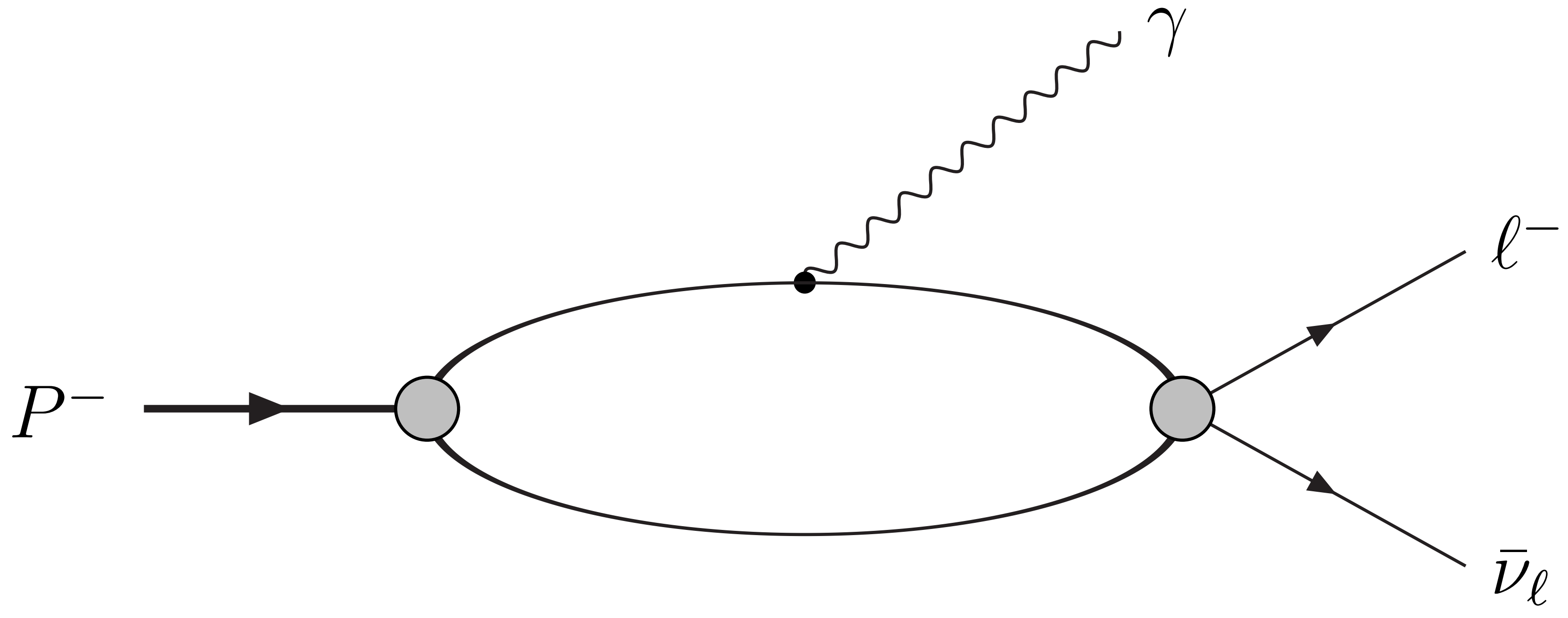


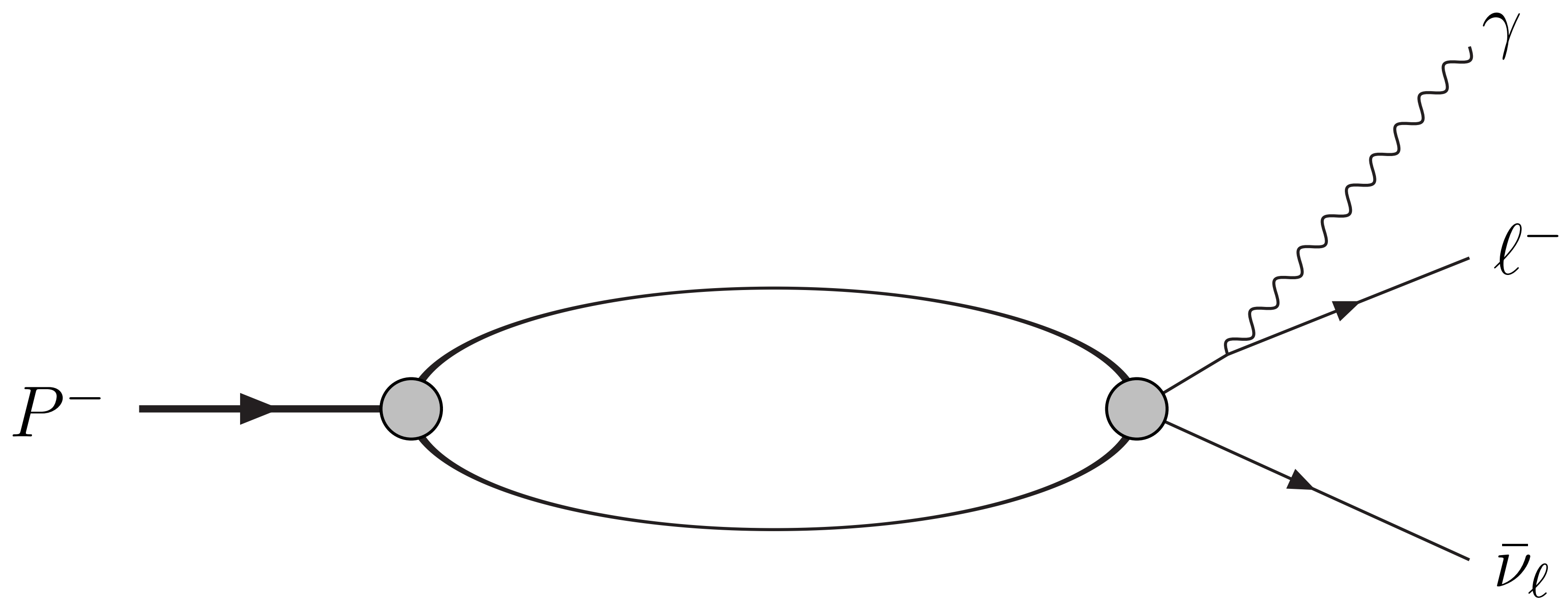


- Non-perturbative contribution to $P \to \ell\bar{\nu}_\ell\gamma$ is encoded in:

$$H_W^{\alpha r}(k,\mathbf{p}) = \epsilon_\mu^r(k)\, H_W^{\alpha\mu}(k,\mathbf{p}) = \epsilon_\mu^r(k) \int d^4y\, e^{ik\cdot y}\,\mathrm{T}\ \langle 0 |\, j_W^\alpha(0)\, j_{\rm em}^\mu(y)\, | P(\mathbf{p})\,\rangle$$

$$= \epsilon_\mu^r(k)\Bigg\{ \frac{H_1}{m_K}\left[k^2 g^{\mu\alpha} - k^\mu k^\alpha\right] + \frac{H_2}{m_K}\,\frac{\left[(p\cdot k - k^2)k^\mu - k^2(p-k)^\mu\right](p-k)^\alpha}{(p-k)^2 - m_K^2}$$

$$-i\frac{F_V}{m_K}\varepsilon^{\mu\alpha\gamma\beta}k_\gamma p_\beta + \frac{F_A}{m_K}\left[(p\cdot k - k^2)g^{\mu\alpha} - (p-k)^\mu k^\alpha\right] + f_P\left[g^{\mu\alpha} - \frac{(2p-k)^\mu(p-k)^\alpha}{(p-k)^2 - m_K^2}\right]\Bigg\}$$

- For decays into a real photon, $k^2 = 0$ and $\varepsilon \cdot k = 0$, only the decay constant $f_P$ and the vector and axial form factors $F_V(x_\gamma)$ and $F_A(x_\gamma)$ are needed to specify the amplitude ($x_\gamma = 2p\cdot k/m_P^2\,,\ 0 < x_\gamma < 1 - m_\ell^2/m_P^2$).

- In phenomenology $F^\pm \equiv F_V \pm F_A$ are more natural combinations.

# Minkowski → Euclidean Continuation

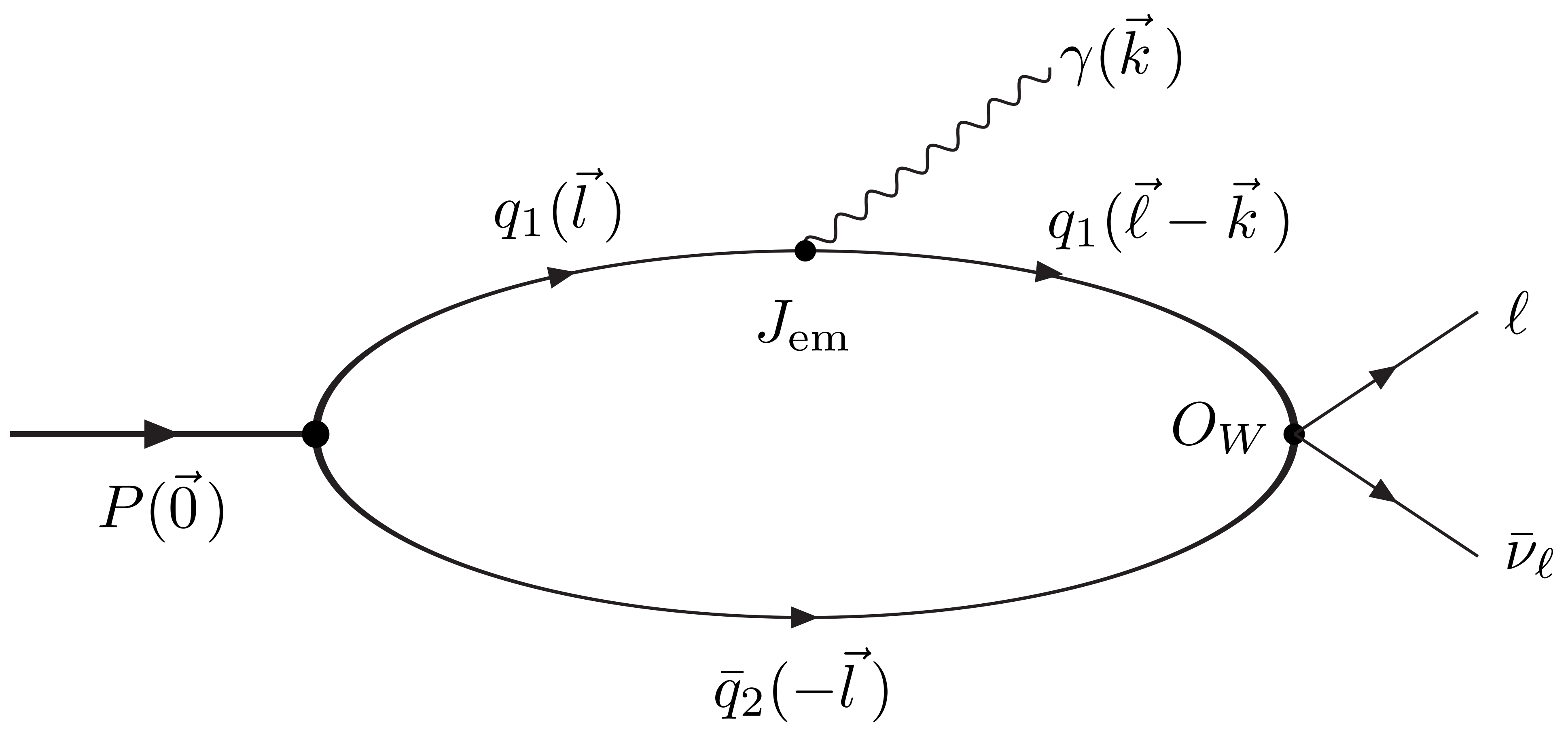


- We assume that $P$ is the lightest particle with quantum numbers $q_1\bar{q}_2$.
- The decay $P \to |n,\gamma\rangle$, where $|n\rangle$ also has quantum numbers $q_1\bar{q}_2$, is therefore not possible.
- The states propagating between $J_{\rm em}$ and $O_W$ can therefore not be on-shell.

- In this case the photon is real, and so there is also no on-shell state which can propagate between $O_W(t_W)$ and $J_{\rm em}(t_{\rm em})$ where $t_{\rm em} > t_W$ .
- As expected, the Minkowski-Euclidean continuation is therefore straightforward.
- This is not the case in general when the emitted photon is virtual.

# Computing the Form Factors

$$H_W^{\alpha r}(k,\mathbf{p}) = \epsilon_\mu^r(k)\, H_W^{\alpha\mu}(k,\mathbf{p}) = \epsilon_\mu^r(k) \int d^4y\, e^{ik\cdot y}\; T\langle 0\,|\, j_W^\alpha(0)\, j_{\rm em}^\mu(y)\,|\,P(\mathbf{p})\rangle$$

- Euclidean Correlation Functions:

$$C_W^{\alpha r}(t;\mathbf{k},\mathbf{p}) = -\,i\epsilon_\mu^r(k)\int d^4y \int d^3x\; e^{t_y E_\gamma - i\mathbf{k}\cdot\mathbf{y}}\, e^{i\mathbf{p}\cdot\mathbf{x}}\; T\langle 0\,|\, j_W^\alpha(t,\mathbf{0})\, j_{\rm em}^\mu(y)\, \phi_P^\dagger(0,\mathbf{x})\,|\,0\rangle$$

- $H_W^{\alpha r}(k,\mathbf{p})$ can be obtained from the large $t$ limit of the correlation function:

$$R_W^{\alpha r}(t;k,\mathbf{p}) \equiv \frac{2E}{e^{-(E-E_\gamma)t}\langle P(\mathbf{p})\,|\,\phi_P^\dagger(0)\,|\,0\rangle}\, C_W^{\alpha r}(t;k,\mathbf{p}) + \cdots$$

where $E = \sqrt{m_P^2 + \mathbf{p}^2}$ .

# Choice of Kinematics

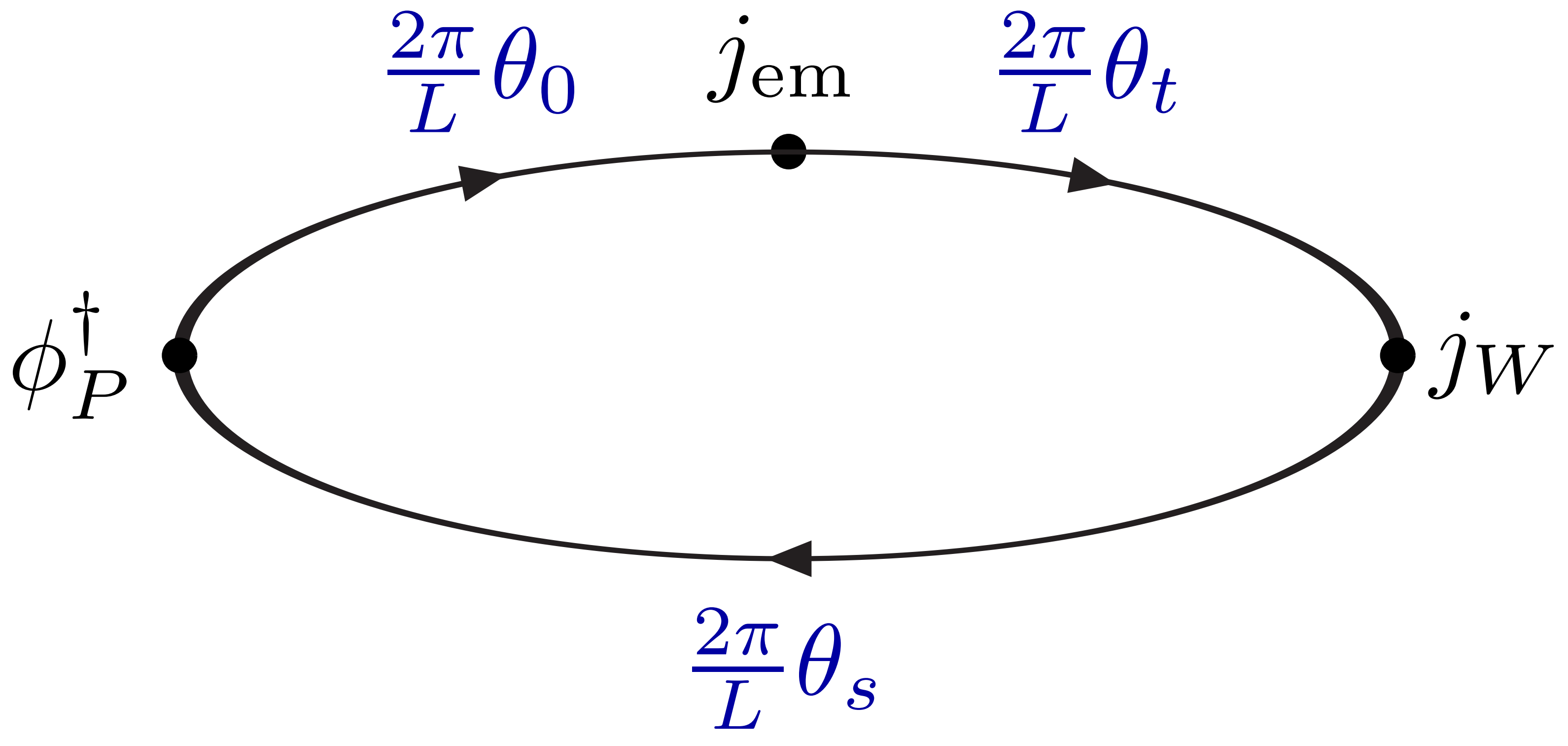


- We use twisted boundary conditions to introduce momenta,

$$\mathbf{p} = \frac{2\pi}{L}(\theta_0 - \theta_s)\,; \qquad \mathbf{k} = \frac{2\pi}{L}(\theta_0 - \theta_t)\,,$$

with both $\mathbf{p}$ and $\mathbf{k}$ in the $z$ direction

$$\mathbf{p} = (0, 0, |\,\mathbf{p}\,|\,)\,; \qquad \mathbf{k} = (0, 0, E_\gamma)\,.$$

- For the polarisation vectors we choose, $\epsilon_\mu^1 = \left(0, -\frac{1}{\sqrt{2}}, -\frac{1}{\sqrt{2}}, 0\right)$, $\epsilon_\mu^2 = \left(0, \frac{1}{\sqrt{2}}, -\frac{1}{\sqrt{2}}, 0\right)$, $\epsilon_\mu^3 = \epsilon_\mu^0 = 0\,.$

- With these choices

$$R_A(t) \equiv \frac{1}{2m_P}\sum_{r=1,2}\sum_{j=1,2}\frac{R^{jr}(t;k,\mathbf{p})}{\epsilon_j^r} \to x_\gamma\, F_A(x_\gamma) + \frac{2f_P}{m_P} \qquad R_V(t) \equiv \frac{m_P}{4}\sum_{r=1,2}\sum_{j=1,2}\frac{R_V^{jr}(t;k,\mathbf{p})}{i\left(E_\gamma\, \epsilon^{\mathbf{r}} \times \mathbf{p} - E\, \epsilon^{\mathbf{r}} \times \mathbf{k}\right)^j} \to F_V(x_\gamma)\,.$$

- Thus in principle the two form factors, $F_V$ and $F_A$ can be determined.

# $\mathrm{P} \to \ell \nu_\ell \gamma$ radiative decays - the form factors

- We have computed $F_V(x_\gamma)$ and $F_A(x_\gamma)$ for $\pi, K, D_{(s)}$ mesons. A.Desiderio et al. arXiv:2006.05358
  - The computations were performed on 11 ETMC $N_f = 2+1+1$ ensembles with 0.062 fm < a <0.089 fm and 227 MeV< $m_\pi$ <441 MeV and a range of volumes.
  - Computations are performed in the electroquenched approximation.

- Our data is fully consistent with a parametrisation of the form :

$$F^P_{A,V}(x_\gamma) = C^P_{A,V} + D^P_{A,V} x_\gamma \,.$$

- Other parametrisation were also tried and presented.

- Values of the parameters are presented in the paper.

- Below we compare our results to the experimental data and also to LO ChPT:

$$F_A(x_\gamma) = \frac{8m_P}{f_P}(L_9^r + L_{10}^r) \simeq \frac{8m_P}{f_P}(0.0017)\,, \qquad F_V(x_\gamma) = \frac{m_P}{4\pi^2 f_p}\,.$$

# Non-perturbative subtractions of IR divergent discretisation effects

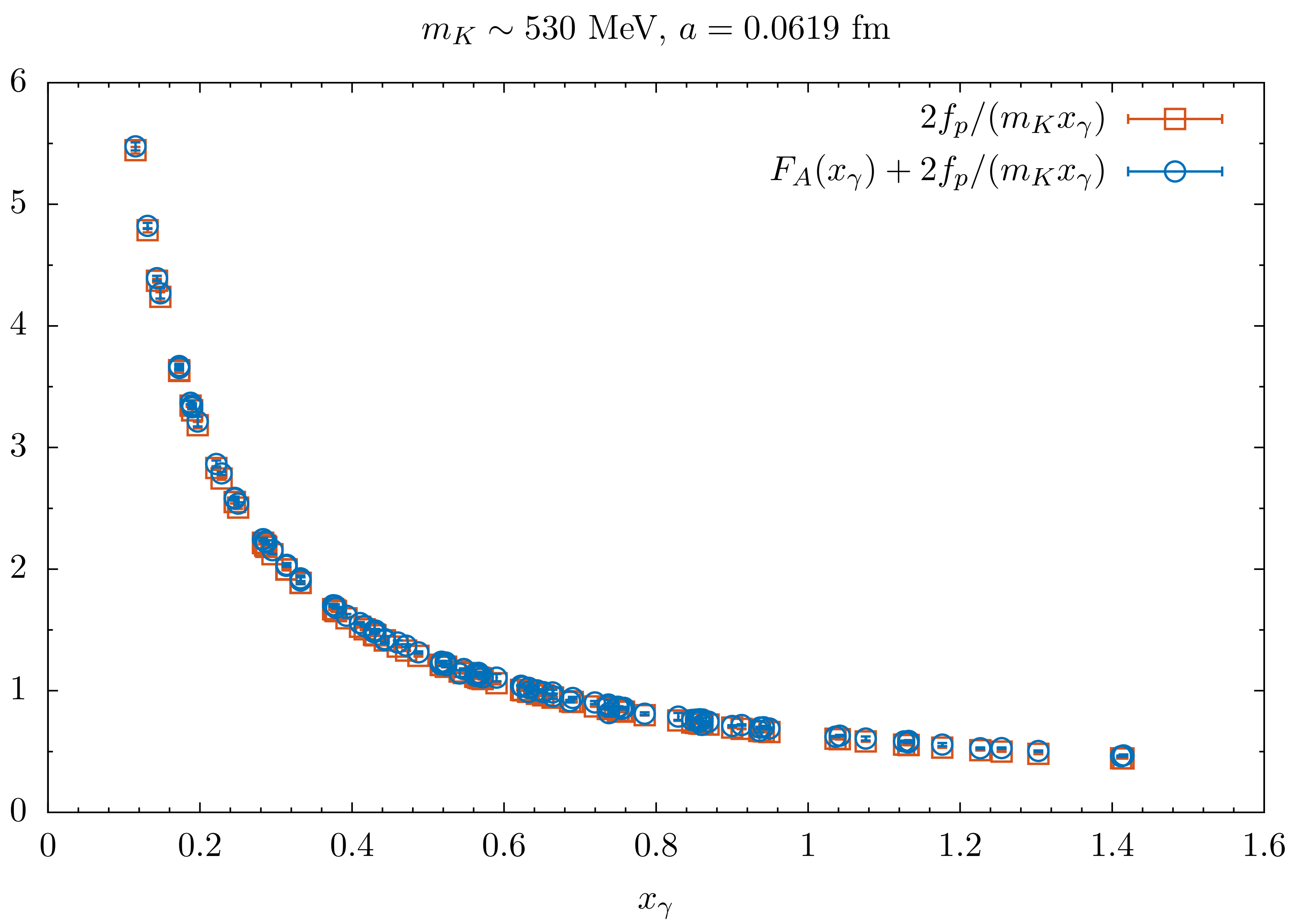


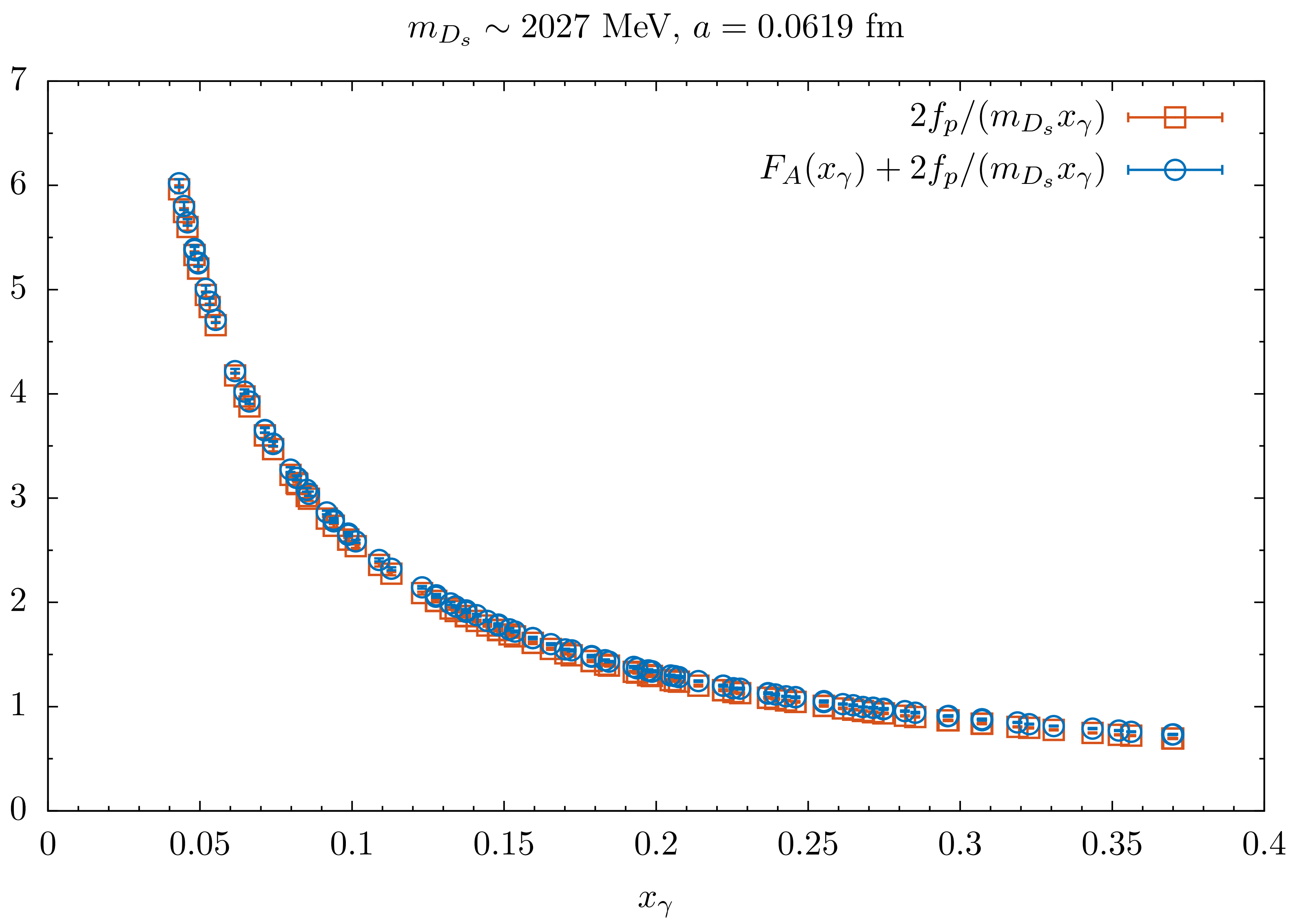


- The combination $F_A(x_\gamma) + 2f_p/(m_P x_\gamma)$ is dominated by $2f_p/(m_P x_\gamma)$, particularly at small $x_\gamma$ .
- We rewrite the behaviour of the axial estimator to include discretisation effects

$$\frac{R_A(t)}{x_\gamma} \to \left[F_A(x_\gamma) + a^2 \Delta F_A(x_\gamma)\right] + \frac{2}{m_P x_\gamma}\left(f_P + a^2 \Delta f_P\right) + \cdots$$

- $f_P$ obtained from two-point functions $\neq (f_P + a^2 \Delta f_P) \Rightarrow$ incomplete cancelation of the infrared divergent term.

- We introduce the modified estimator

$$\bar{R}_A(t) = e^{-tE_\gamma} \frac{\sum_{r=1,2} \sum_{j=1,2} \frac{R^{jr}(t; k, \mathbf{p})}{\epsilon_j^r}}{\sum_{r=1,2} \sum_{j=1,2} \frac{R^{jr}(t; 0, \mathbf{p})}{\epsilon_j^r}} - 1$$

$$\frac{2f_P}{m_P x_\gamma} \bar{R}_A(t) \to F_A^{\mathrm{NPsub}}(x_\gamma) = F_A(x_\gamma) + O(a^2)\,.$$

# Non-perturbative subtractions of IR divergent discretisation effects (cont.)

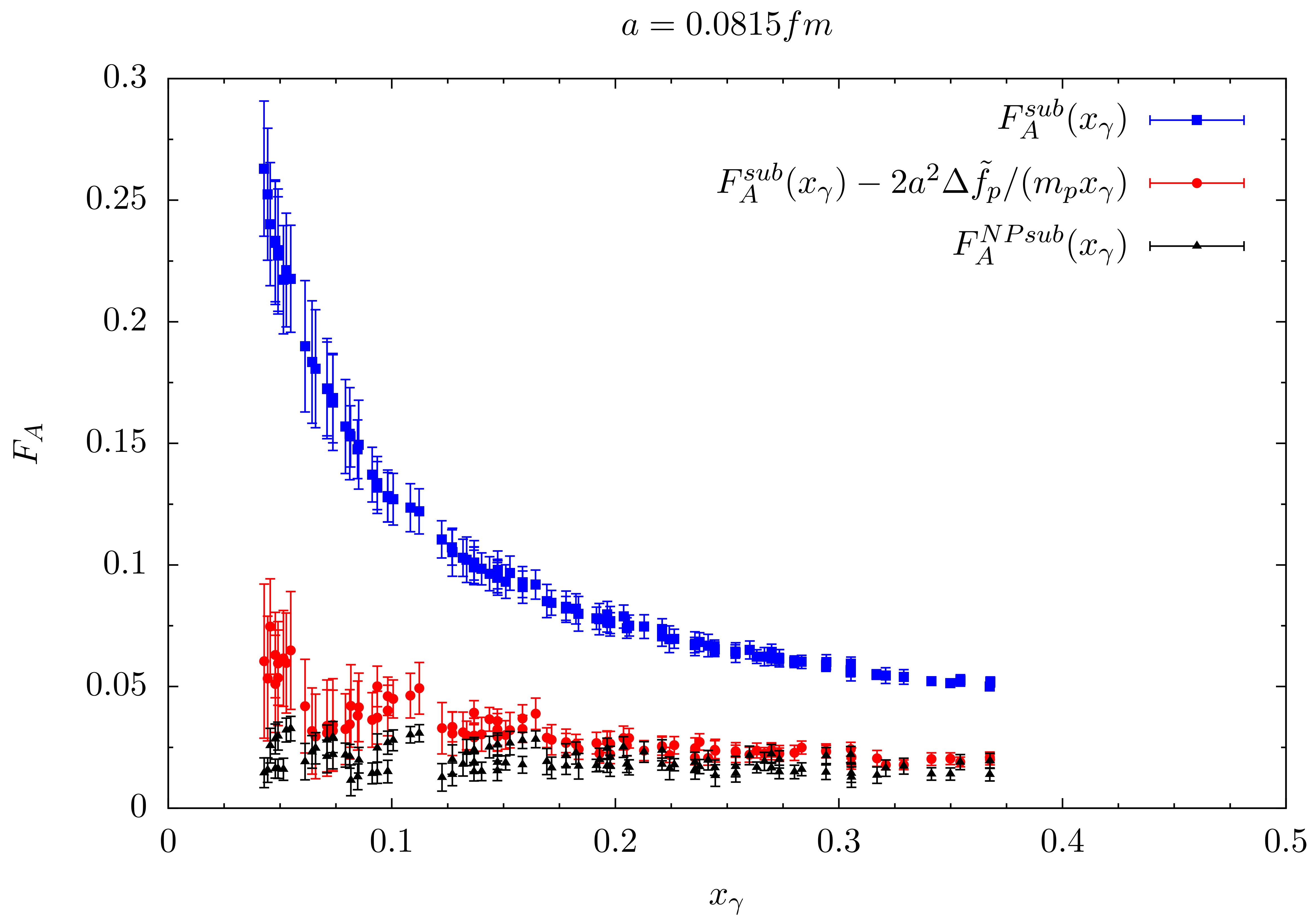


- Blue points - $F_A(x_\gamma)$ obtained by performing the subtraction using the value of $f_P$ obtained from two-point correlation functions.
- Red Points - Discretisation effects in $f_P$ fitted and subtracted.
- Black Points - $F_A^{\mathrm{NPsub}}(x_\gamma)$

- Illustrative example: $F_A(x_\gamma)$ for the $D_s$ meson.

# Comparison with Experimental Data

R.Frezzotti, M.Garofalo, V.Lubicz, G.Martinelli, CTS, F.Sanfilippo, S.Simula and N.Tantalo, arXiv:2012.02120

- $K \to e\nu_e\gamma$ KLOE, arXiv:0907.3594
  J-PARC E36, arXiv:2107.03583
  NA62, arXiv:2???.?????

- $K \to \mu\nu_\mu\gamma$ E787@BNL AGS, hep-ex/0003019
  ISTRA+ @U-79 Protvino, arXiv:1005.3517
  OKA@U-79 Protvino, arXiv:1904.10078

- $\pi \to e\nu_e\gamma$ PIBETA@$\pi$E1 beam line PSI, arXiv:0804.1815

- The different experiments introduce different cuts on $E_\gamma$, $E_\ell$ and $\cos\theta_{\ell\gamma}$, resulting in sensitivities to different form factors.

# Comparison with Experimental Data — Kaon Decays

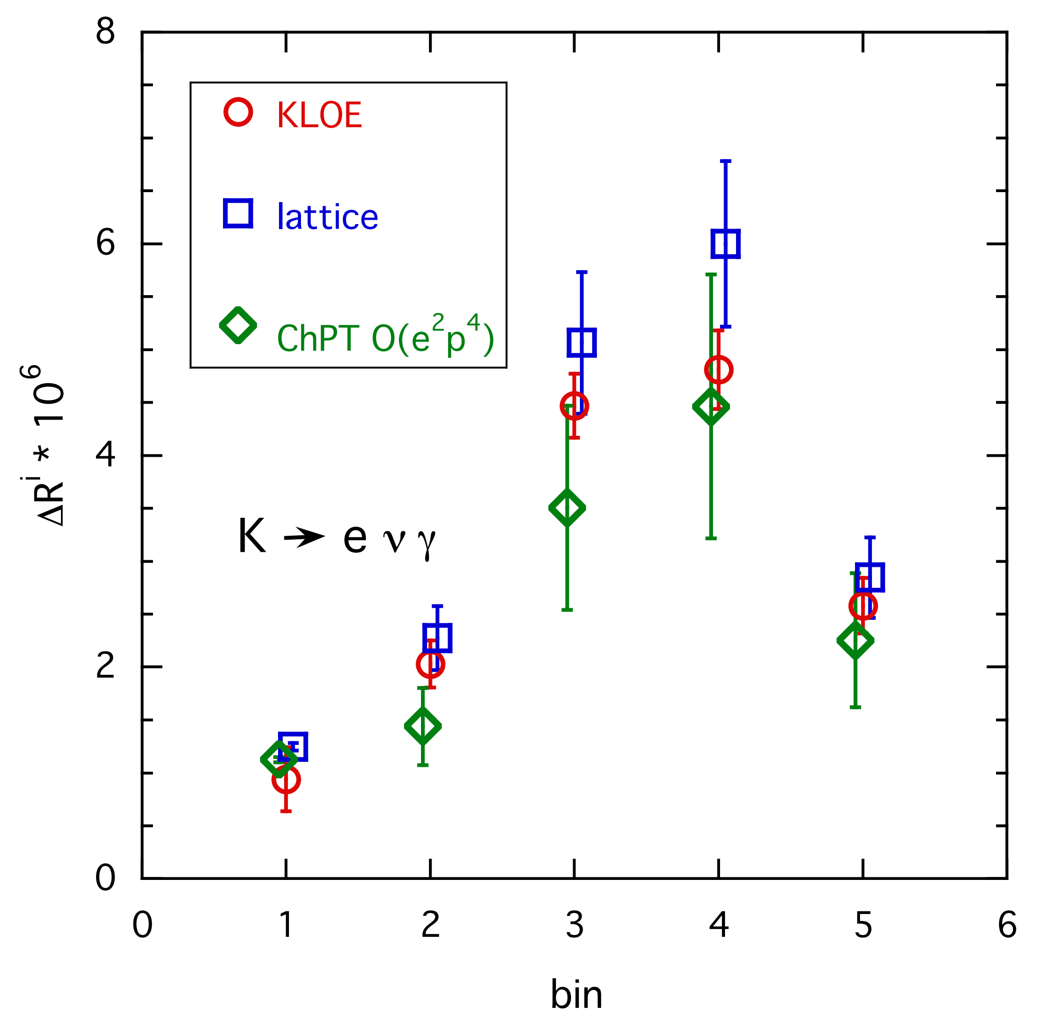


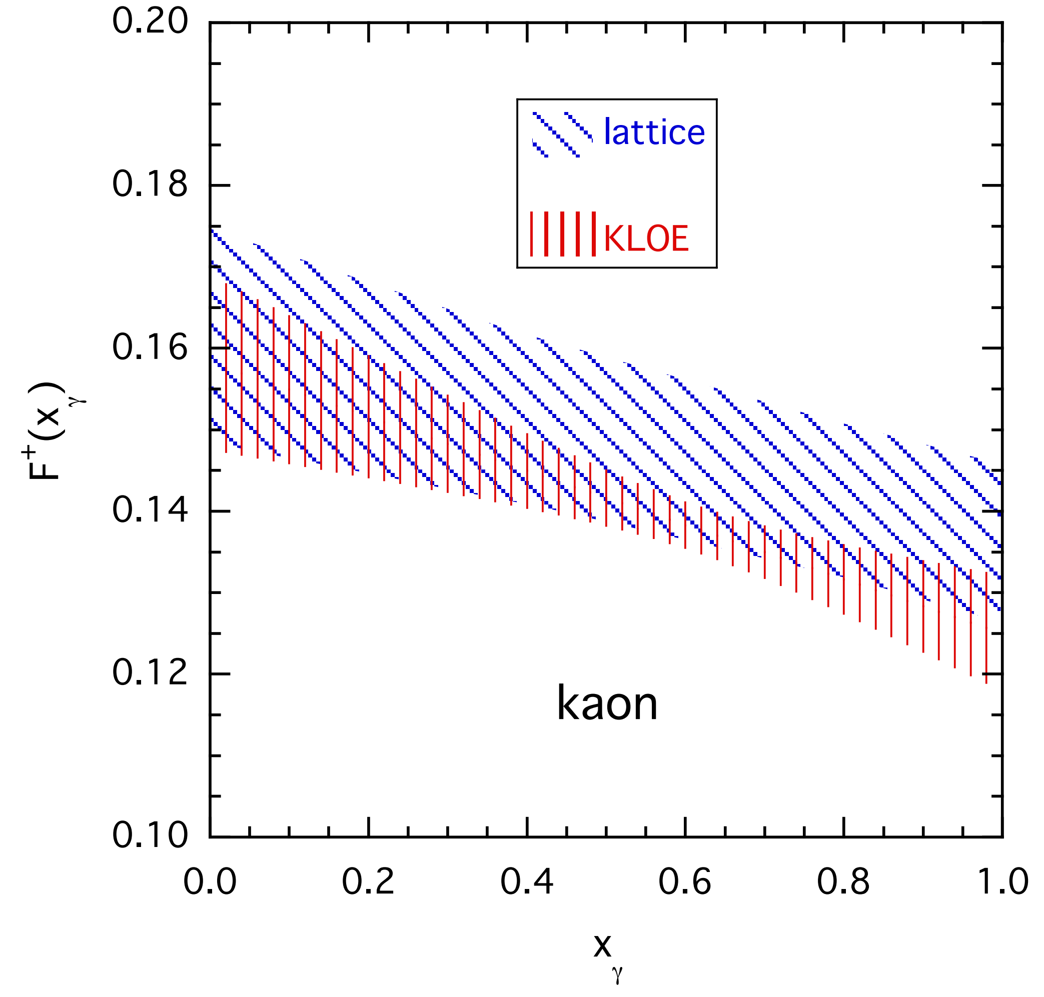


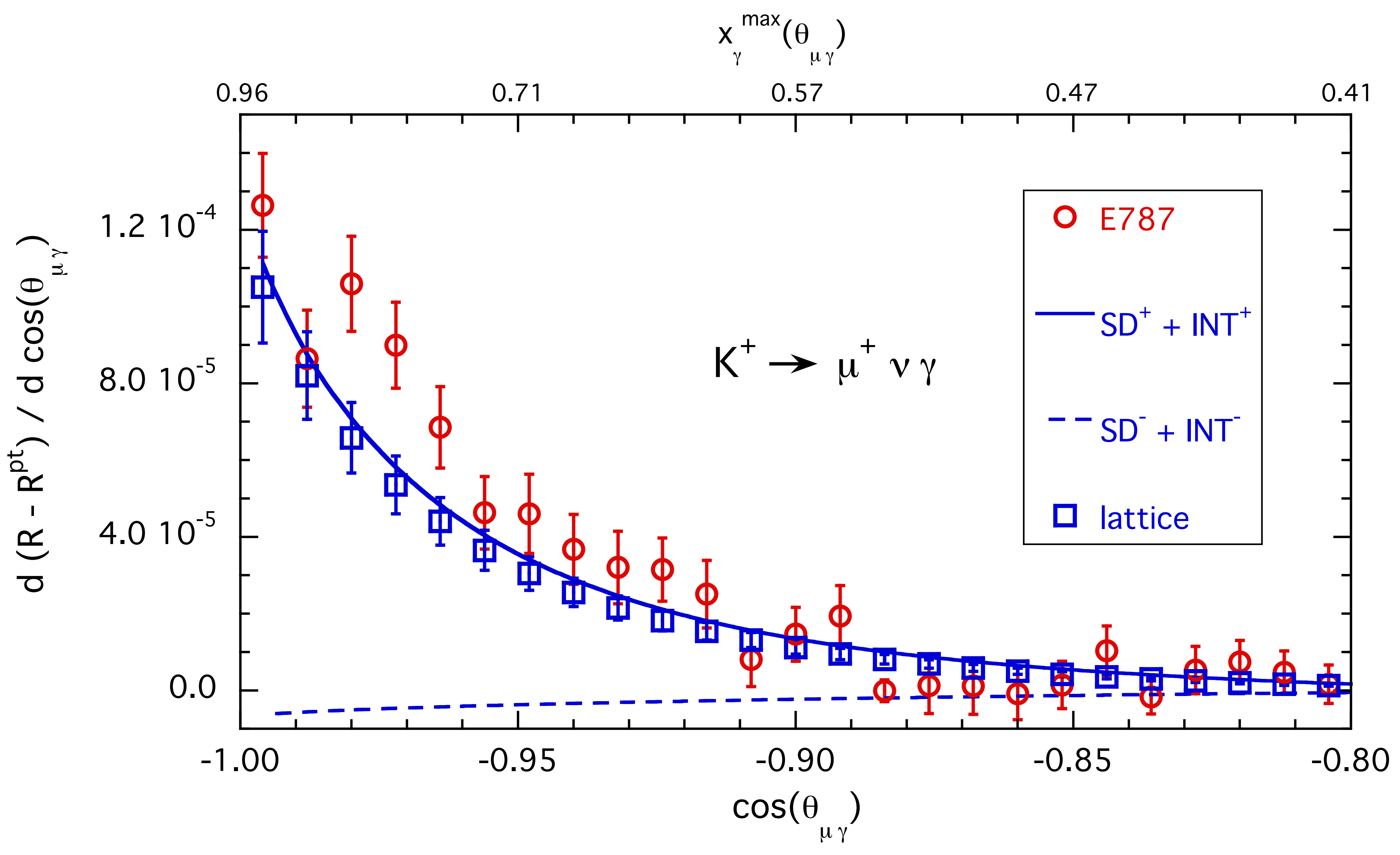


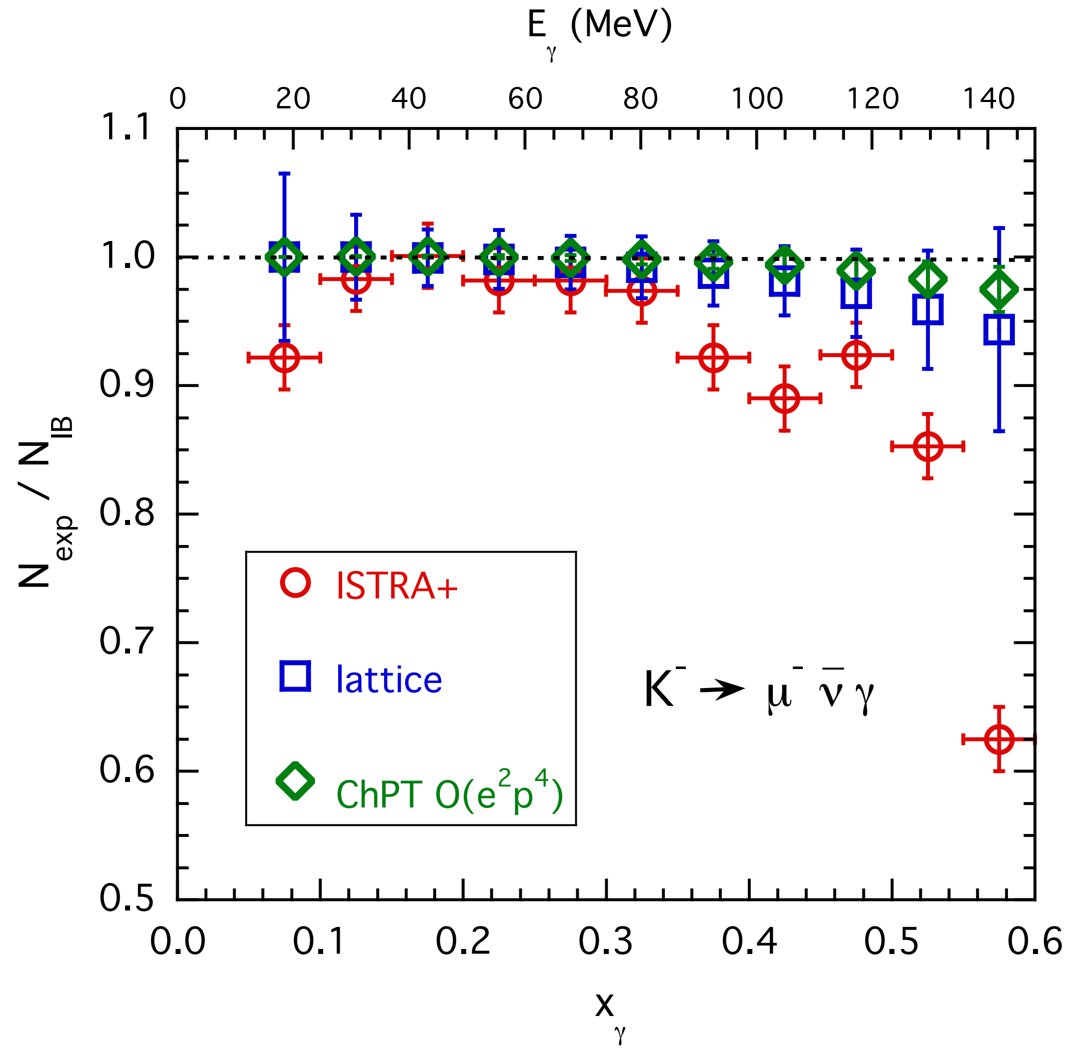


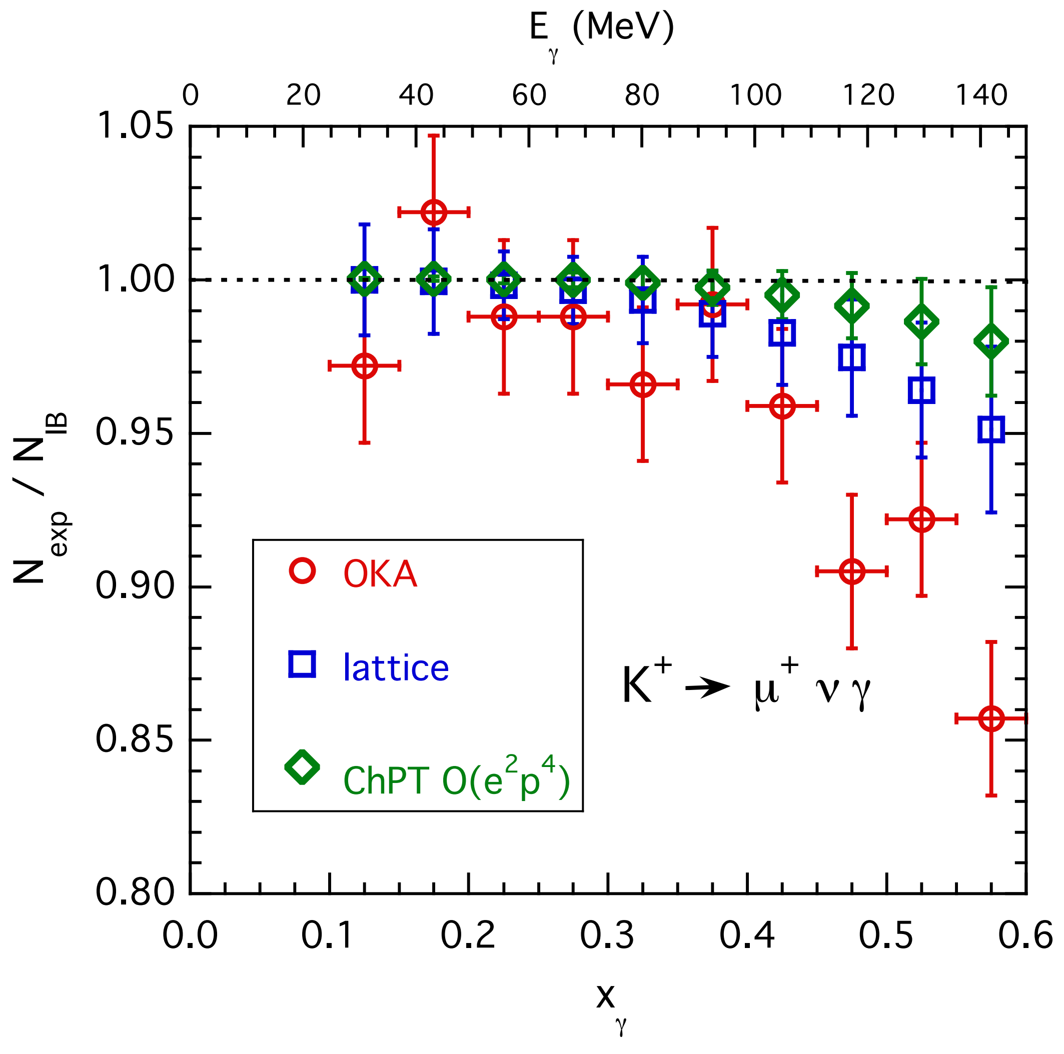


- Good Agreement with KLOE
- Significant tensions with $K \to \mu\nu_\mu\gamma$ experiments
- Unable to find a set of phenomenological form factors to account for all the data.
- NA62 will soon have the most precise results for $K \to e\nu_e\gamma$ decay rates.
- Is it conceivable that we have LFU-violation here?

# Comparing JPARC and KLOE's Results

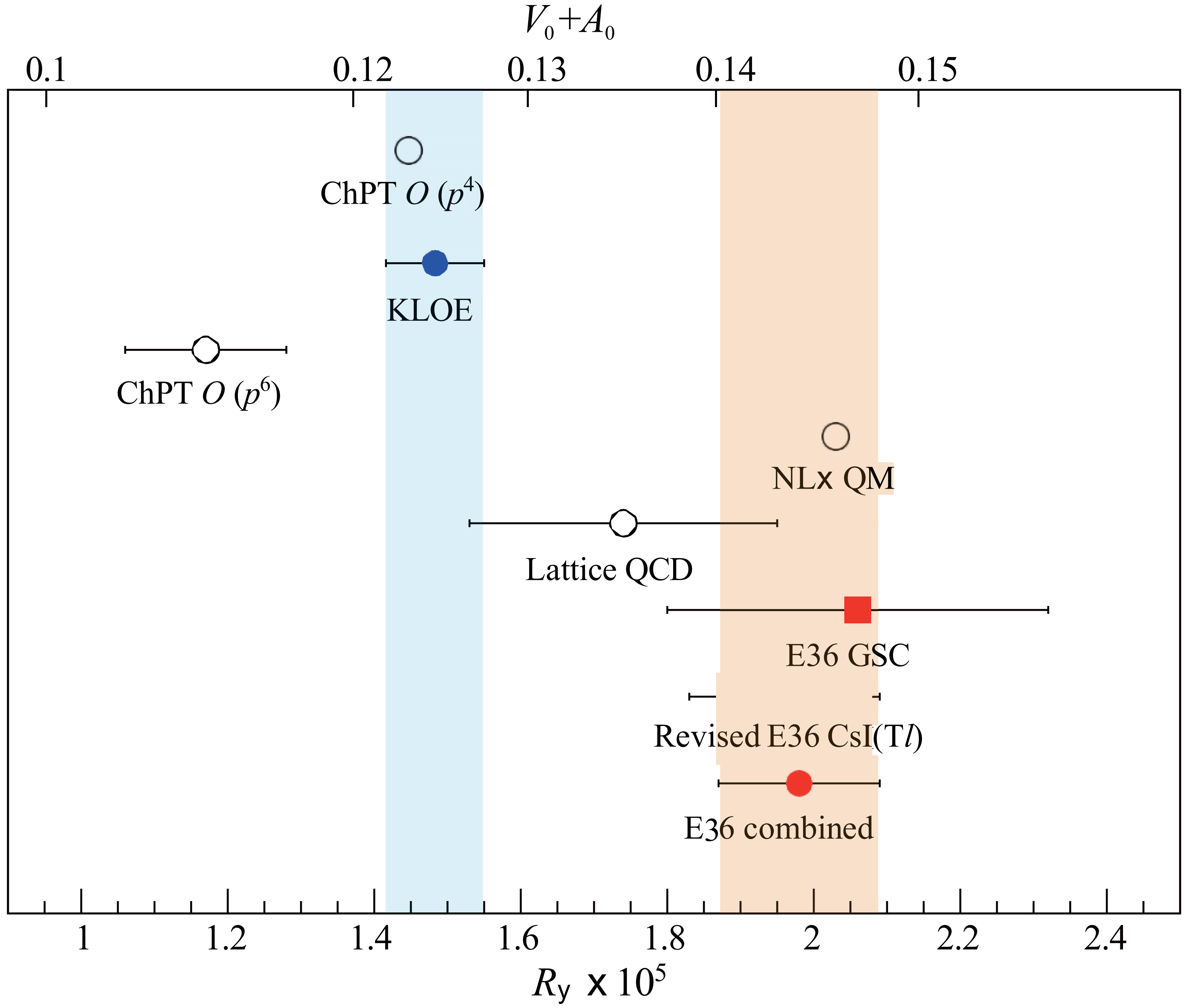


J-PARC E36 Collaboration, A.Kobayashi et al., arXiv:2212.10702

| $E_\gamma$ (MeV) | $p_e$ (MeV) | KLOE [10] | J-PARC E36 [11] | lattice [9] | ChPT |
|---|---|---|---|---|---|
| 10 - 250 | > 200 | 1.483 ± 0.066 ± 0.013 | 1.85 ± 0.11 ± 0.07 | 1.743 ± 0.212 | 1.279 ± 0.324 |

(Units of $10^{-5}$)

S.Simula et al., PoS Lattice 2021 (2022) 631

- E36 Result was subsequently updated to $(1.98 \pm 0.11) \times 10^{-5}$ (as in the figure above).

# Comparison with Experimental Data — Pion Decays

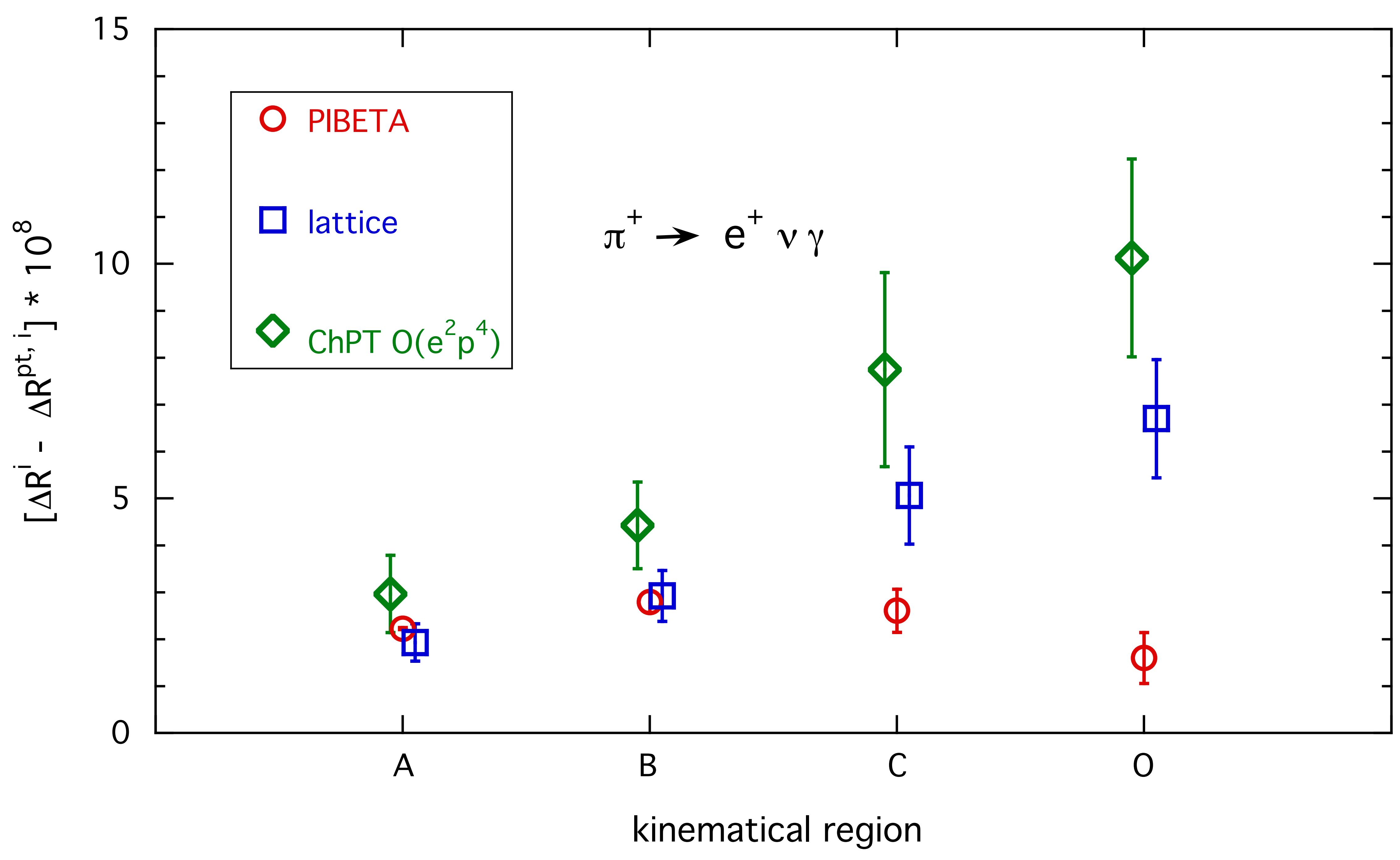


$$\theta_{e\gamma} > 40^\circ$$

- A: $E_\gamma > 50\,\mathrm{MeV}$ and $E_e > 50\,\mathrm{MeV}$
- B: $E_\gamma > 50\,\mathrm{MeV}$ and $E_e > 10\,\mathrm{MeV}$
- C: $E_\gamma > 10\,\mathrm{MeV}$ and $E_e > 50\,\mathrm{MeV}$
- D: $E_\gamma > 10\,\mathrm{MeV}$ and $E_e > m_e$

- It is also difficult to understand the PIBETA data in some kinematical regions.

# $D_s$ Decays

- In the paper discussed above, we have also computed the form factors for the $D_s$ meson but only for $E_\gamma < 0.4\,\text{GeV}$ .

- In a subsequent paper we have computed them over the full kinematic range.

R.Frezzotti, G.Gagliardi, V.Lubicz, G.Martinelli, F.Mazzetti, CTS, F.Sanfilippo, S.Simula, and N.Tantalo, arXiv:2306.05904

- The calculations were performed using four ETMC ensembles with $a \in [0.058, 0.09]\,\text{fm}$ , three of which have approximately physical pion masses and the coarsest has $m_\pi = 174.5\,\text{MeV}$ .
  - Sea Quarks - Wilson Clover TM Fermions and maximal twist
  - Valence Quarks - Osterwalder-Seiler Fermions
  - Physical $m_s$ and $m_c$.

# $D_s \to \ell \nu_\ell \gamma$ - Results for the Form Factors

| $x_\gamma$ | $F_A$ | $\Delta F_A$ | $F_V$ | $\Delta F_V$ |
|---|---|---|---|---|
| 0.1 | 0.0813 | 0.0054 | -0.1048 | 0.0097 |
| 0.2 | 0.0715 | 0.0041 | -0.0819 | 0.0028 |
| 0.3 | 0.0641 | 0.0033 | -0.0643 | 0.0013 |
| 0.4 | 0.0582 | 0.0028 | -0.0519 | 0.0008 |
| 0.5 | 0.0534 | 0.0021 | -0.0431 | 0.0008 |
| 0.6 | 0.0495 | 0.0024 | -0.0363 | 0.0008 |
| 0.7 | 0.0463 | 0.0031 | -0.0316 | 0.0007 |
| 0.8 | 0.0432 | 0.0032 | -0.0291 | 0.0010 |
| 0.9 | 0.0433 | 0.0083 | -0.0297 | 0.0056 |
| 1.0 | 0.0489 | 0.0229 | -0.0315 | 0.0152 |

- Appendix A for an explanation of why the errors grow at large $x_\gamma$.
- Discussion of method to reduce such errors studied in

Davide Giusti's Talk
D.Giusti et al., arXiv:2302.01298

- Our Results for the form factors are well represented by the following VMD-inspired ansatz:

$$F_W(x_\gamma) = \frac{C_W}{\sqrt{R_W^2 + x_\gamma^2/4}\left(\sqrt{R_W^2 + x_\gamma^2/4} + x_\gamma/2 - 1\right)} + B_W$$

where $W = A, V$ and $R_W$, $B_W$ and $C_W$ are fit parameters.

- For single pole dominance $R_W = m_{\rm res}/m_{D_s}$ and $B_W = 0$.

- For $F_V$ we obtain stable results for $C_V$, and hence deduce the coupling $g_{D_s^* D_s \gamma}$ using

$$C_V = -\frac{m_{D_s^*} f_{D_s^*} g_{D_s^* D_s \gamma}}{2 m_{D_s}}$$

and $f_{D_s^*} = 268.6(6.6)$ MeV.

ETM Collaboration , V.Lubicz et al., arXiv 1707.04529

# Cancellation in $F_V = F_V^{(c)} + F_V^{(s)}$

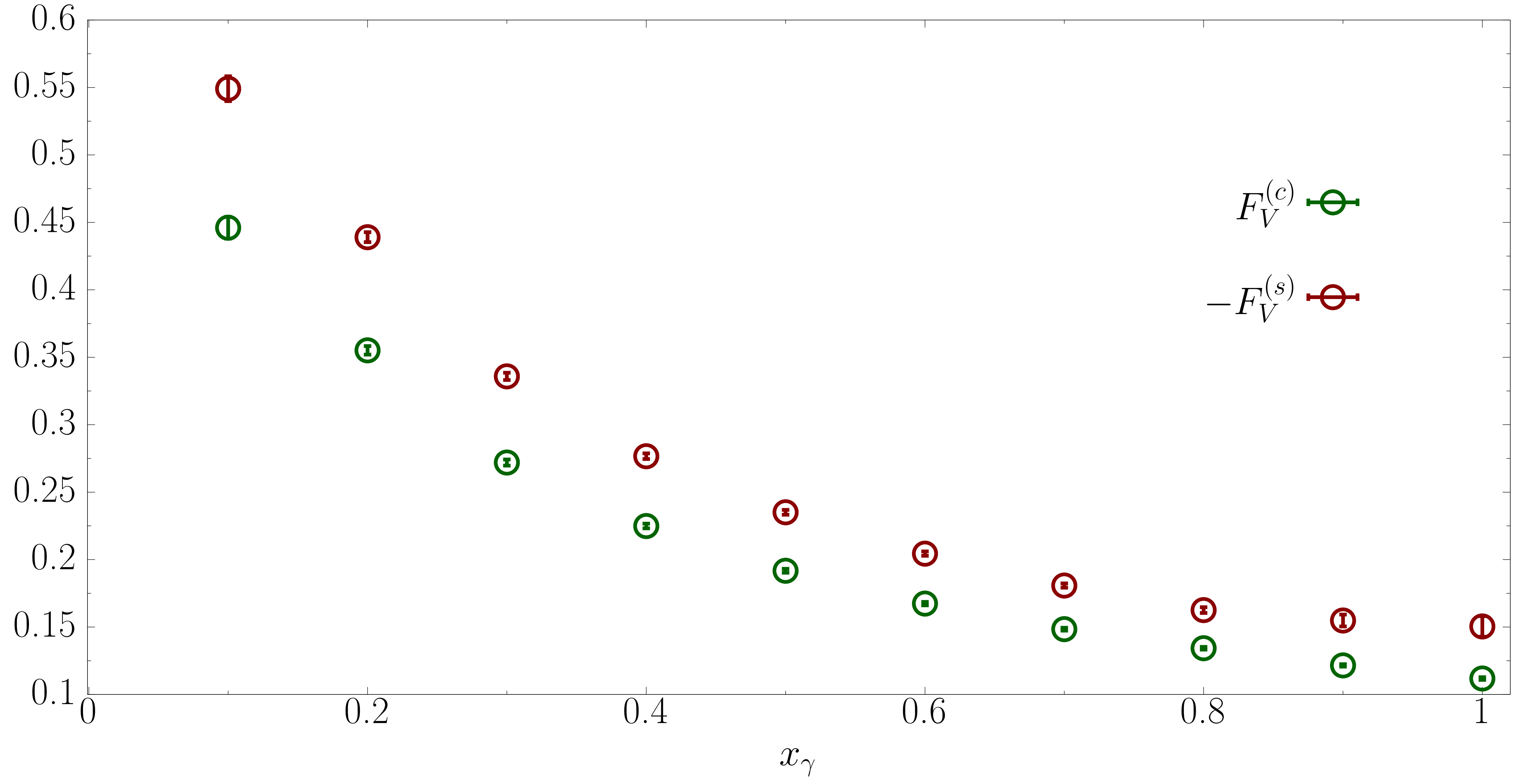


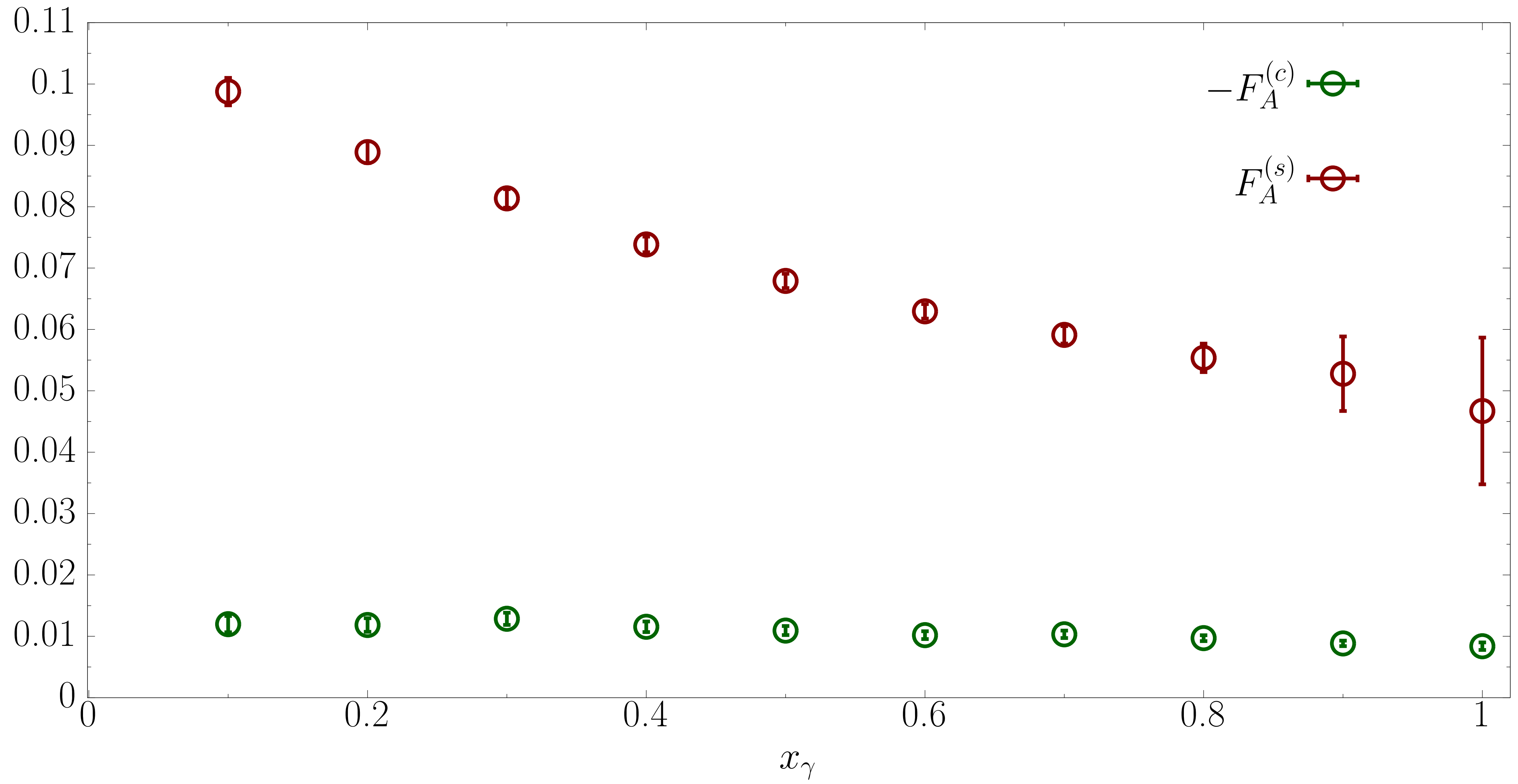


- There is a significant partial cancellation in $F_V$ between the contributions from the emission of the photon from the strange and charm quarks.

- This had been observed previously by the HPQCD collaboration in their computation of the $D_s^* \to D_s\gamma$ decay amplitude. HPQCD Collaboration , arXiv:1312.5264

| | LCSR | HPQCD | This work |
|---|---|---|---|
| $g_{D_s^* D_s\gamma}$ | 0.60(19) | 0.10(2) | 0.118(13) |
| $g^{(s)}_{D_s^* D_s\gamma}$ | 1.0 | 0.50(3) | 0.532(15) |
| $g^{(c)}_{D_s^* D_s\gamma}$ | -0.4 | -0.40(2) | -0.415(16) |
| $g^{(s)}_{D_s^* D_s\gamma}/g^{(c)}_{D_s^* D_s\gamma}$ | -2.5 | -1.25(10) | -1.282(61) |

- $g_{D_s^* D_s\gamma}$ in $\mathrm{GeV}^{-1}$

LCSR = B.Pullin and R.Zwicky, arXiv:2106.13617

# $\mathrm{D_s} \to \ell \nu_\ell \gamma$ — Conclusions

- We find $B(D_s \to e\nu_e\gamma) = 4.4(3) \times 10^{-6}$ for $E_\gamma > 10\,\mathrm{MeV}$ in the rest frame of the $D_s$ meson. This is consistent with the corresponding bound $B(D_s \to e\nu_e\gamma) < 1.3 \times 10^{-4}$ at 90% confidence level from BESIII (quoted in PDG).

- Even for photon energies as low as $10\,\mathrm{MeV}$, we find that the Structure Dependent contribution dominates the branching fraction because of the strong helicity suppression of the point-like term by a factor of $(m_e/m_{D_s})^2$.
  - Such radiative decays therefore provide excellent test of the SM and Beyond.

- We use our results to test the validity and applicability of model dependent calculations.
  - LCSR calculations at NLO fail to reproduce our results for the form factors.

    B.Pullin and R.Zwicky, arXiv:2106.13617, J.Lyon and R.Zwicky, arXiv:1210.6546
  - Pure VMD parametrisation does not always reproduce the momentum dependence of the form factors.
  - There are also quark model predictions for the branching ratio in the range $10^{-3} - 10^{-5}$.

# 3. The $B_s \to \mu^+\mu^-\gamma$ Decay Rate at Large $q^2$

R.Frezzotti, **G.Gagliardi,** V.Lubicz, G.Martinelli, CTS, F.Sanfilippo, S.Simula, N.Tantalo, arXiv:2402.03262

- I use this interesting FCNC process to illustrate the elements which we are able to compute and to highlight the important theoretical issues which we are still working to resolve.
    - Preview: We can compute the dominant contribution, but are working to solve the problems which will enable an improved precision.

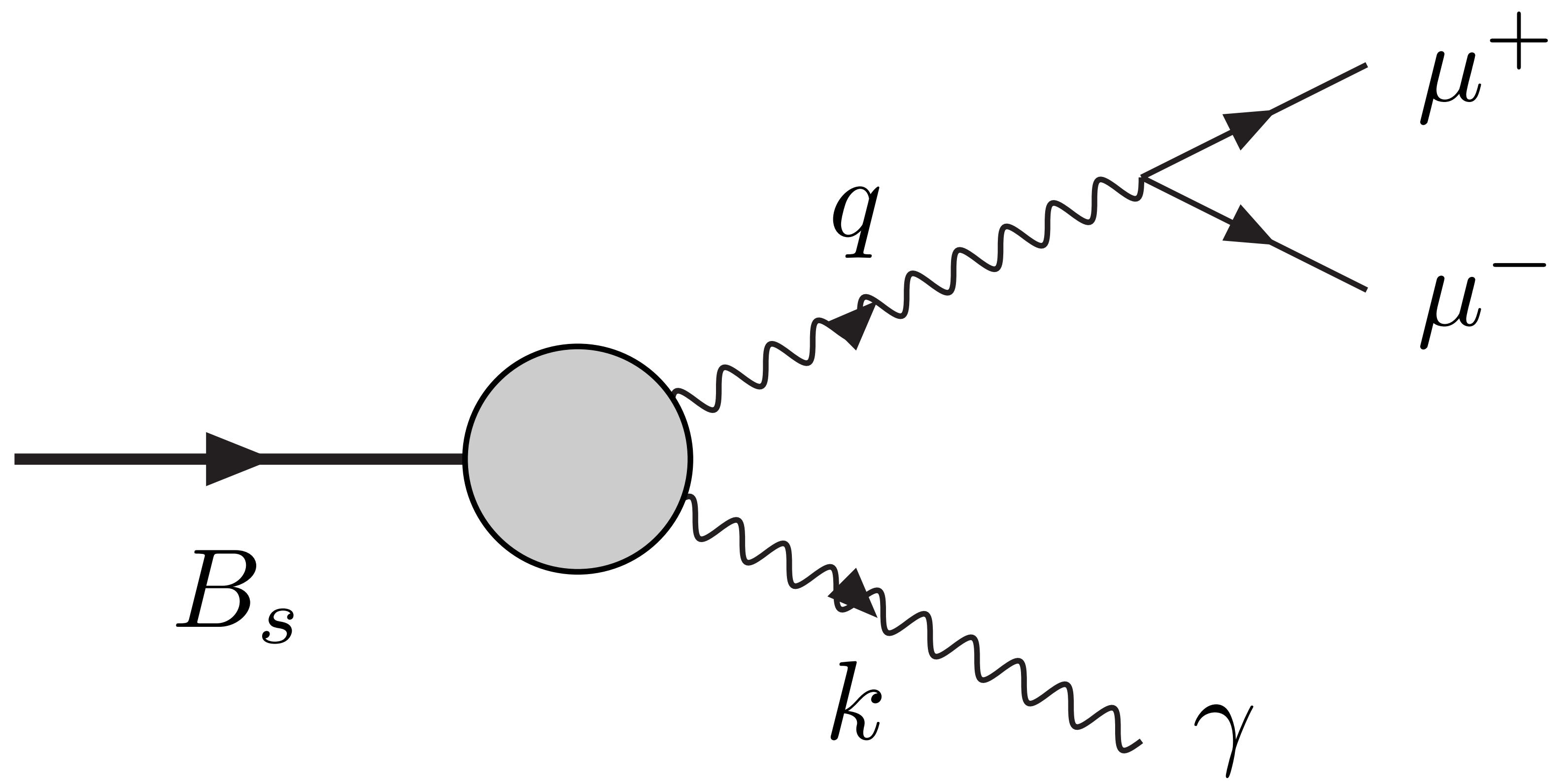


$x_\gamma = \dfrac{2E_\gamma}{m_{B_s}}$, $E_\gamma$ is the energy of the real photon in rest frame of the $B_s$ meson.

$$q^2 = m_{B_s}^2(1 - x_\gamma), \qquad 0 \le x_\gamma \le 1 - \frac{4m_\mu^2}{m_{B_s}^2}$$

- LHCb: $B(B_s \to \mu^+\mu^-\gamma)\,|_{\sqrt{q^2}>4.9\,\mathrm{GeV}} < 2.0 \times 10^{-9}$, arXiv:2108.09283/4

# From the May/June 2024 issue of the Cern Courier

# LHCb targets rare radiative decay

Rare radiative b-hadron decays are powerful probes of the Standard Model (SM) sensitive to small deviations caused by potential new physics in virtual loops. One such process is the decay of $B^0_s \to \mu^+\mu^-\gamma$. The dimuon decay of the $B^0_s$ meson is known to be extremely rare and has been measured with unprecedented precision by LHCb and CMS. While performing this measurement, LHCb also studied the $B^0_s \to \mu^+\mu^-\gamma$ decay, partially reconstructed due to the missing photon, as a background component of the $B^0_s \to \mu^+\mu^-$ process and set the first upper limit on its branching fraction to $2.0 \times 10^{-9}$ at 95% CL (red arrow in figure 1). However, this search was limited to the high-dimuon-mass region, whereas several theoretical extensions of the SM could manifest themselves in lower regions of the dimuon-mass spectrum. Reconstructing the photon is therefore essential to explore the spectrum thoroughly and probe a wide range of physics scenarios.

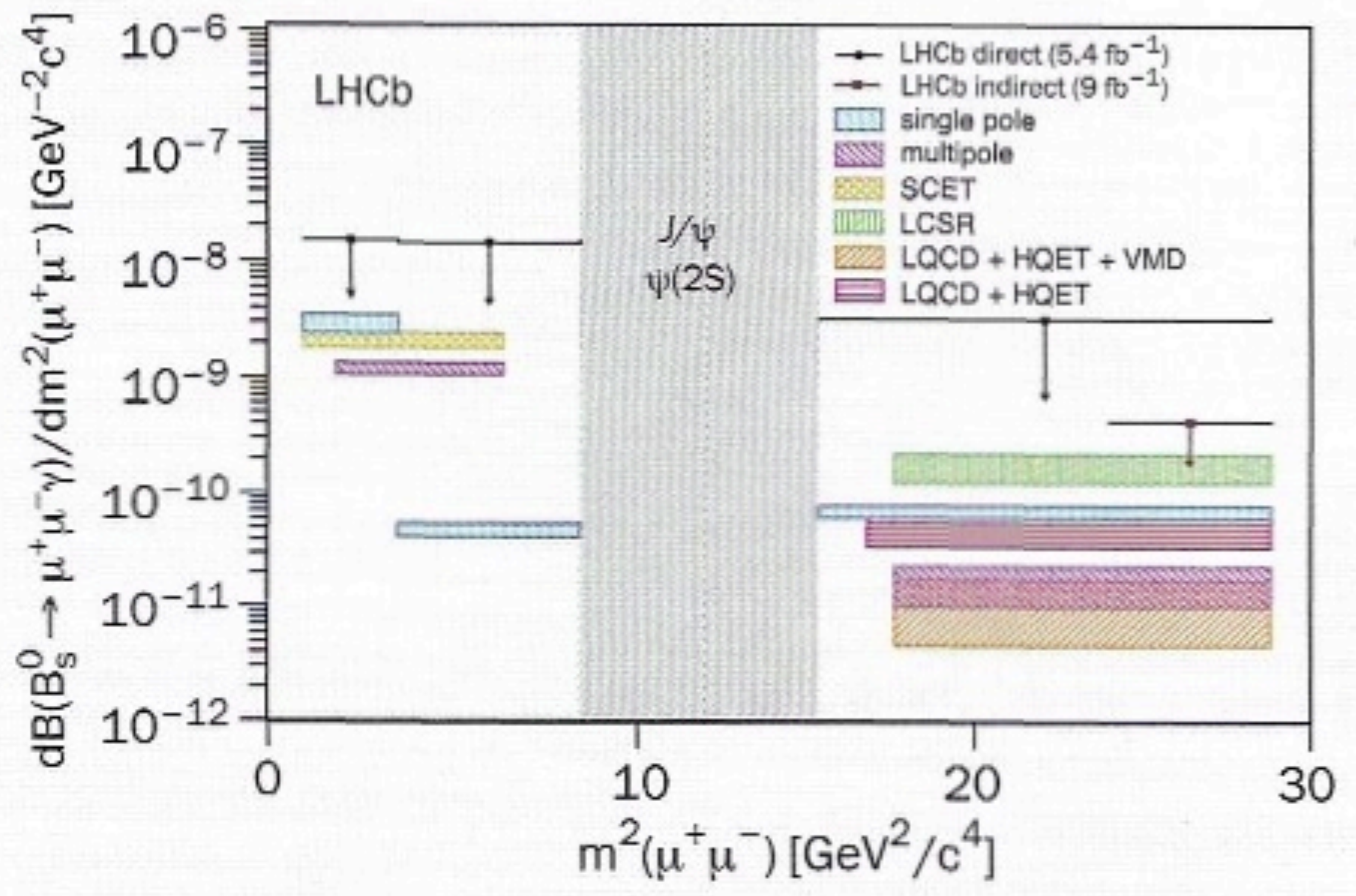


Source: LHCb

**Fig. 1.** *95% confidence limits on differential branching fractions for $B^0_s \to \mu^+\mu^-\gamma$ in intervals of dimuon mass squared ($q^2$). The shaded boxes illustrate SM predictions for the process, according to different calculations.*

The LHCb collaboration now reports the first search for the $B^0_s \to \mu^+\mu^-\gamma$ decay with a reconstructed photon, exploring the full dimuon mass spectrum. Photon reconstruction poses additional experimental challenges, such as degrading the mass resolution of the $B^0_s$ candidate and introducing additional background contributions. To cope with this ambitious search, machine-learning algorithms and new variables have been specifically designed with the aim of discriminating the signal among background processes with similar signatures. The analysis ▷

# The Effective b $\to$ s Hamiltonian

$$\mathcal{H}_{\text{eff}}^{b\to s} = 2\sqrt{2}G_F V_{tb}V_{ts}^* \left[\sum_{i=1,2} C_i O_i^c + \sum_{i=3}^{6} C_i O_i + \frac{\alpha_{\text{em}}}{4\pi}\sum_{i=7}^{10} C_i O_i\right]$$

$$O_1^c = (\bar{s}_i \gamma^\mu P_L c_j)\,(\bar{c}_j \gamma_\mu P_L b_i) \qquad O_2^c = (\bar{s}\,\gamma^\mu P_L c)\,(\bar{c}\,\gamma_\mu P_L b)$$

$$\left(P_{L,R} = \frac{1}{2}(1 \mp \gamma^5)\right)$$

$O_{3-6}$ are QCD Penguins with small Wilson Coefficients

$$O_7 = -\frac{m_b}{e}(\bar{s}\sigma^{\mu\nu} F_{\mu\nu} P_R b) \qquad O_8 = -\frac{g_s m_b}{4\pi\alpha_{\text{em}}}(\bar{s}\sigma^{\mu\nu} G_{\mu\nu} P_R b)$$

$F_{\mu\nu}$ and $G_{\mu\nu}$ are the QED and QCD Field Strength Tensors

$$O_9 = (\bar{s}\,\gamma^\mu P_L b)\,(\bar{\mu}\,\gamma_\mu\,\mu) \qquad O_{10} = (\bar{s}\,\gamma^\mu P_L b)\,(\bar{\mu}\,\gamma_\mu \gamma^5\,\mu)$$

The amplitude is given by: $\mathcal{A} = \langle\, \gamma(k,\epsilon)\,\mu^+(p_1)\,\mu^-(p_2)\,|\,-\mathcal{H}_{\text{eff}}^{b\to s}\,|\,B_s(p)\,\rangle_{\text{QCD+QED}}$

$$= -e\frac{\alpha_{\text{em}}}{\sqrt{2}\pi} V_{tb}\,V_{ts}^*\,\epsilon_\mu^* \left[\sum_{i=1}^{9} C_i\,H_i^{\mu\nu} L_{V\,\nu} + C_{10}\left(H_{10}^{\mu\nu} L_{A\,\nu} - i\frac{f_{B_s}}{2}L_A^{\mu\nu} p_\nu\right)\right]$$

The $H^{\mu\nu}$ and $L$ are hadronic and leptonic tensors respectively

# Contribution from "Semileptonic" Operators - $F_V$ and $F_A$

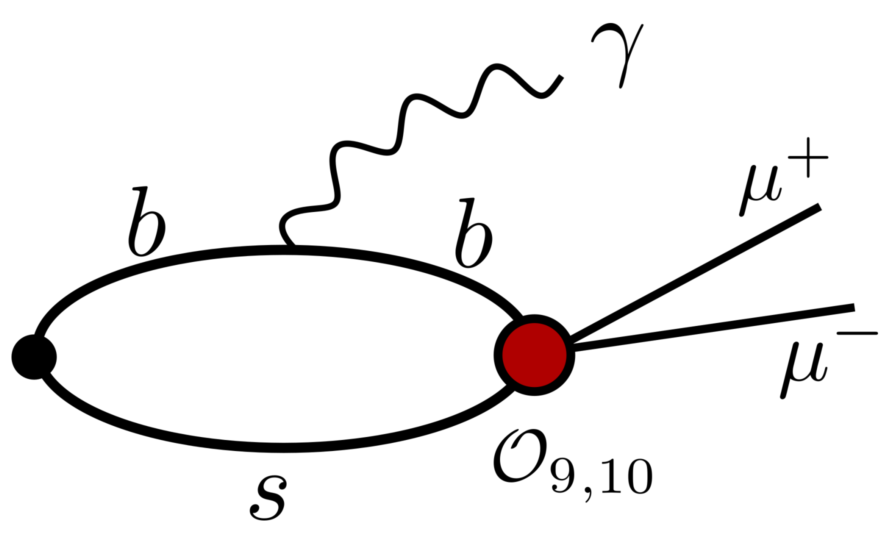


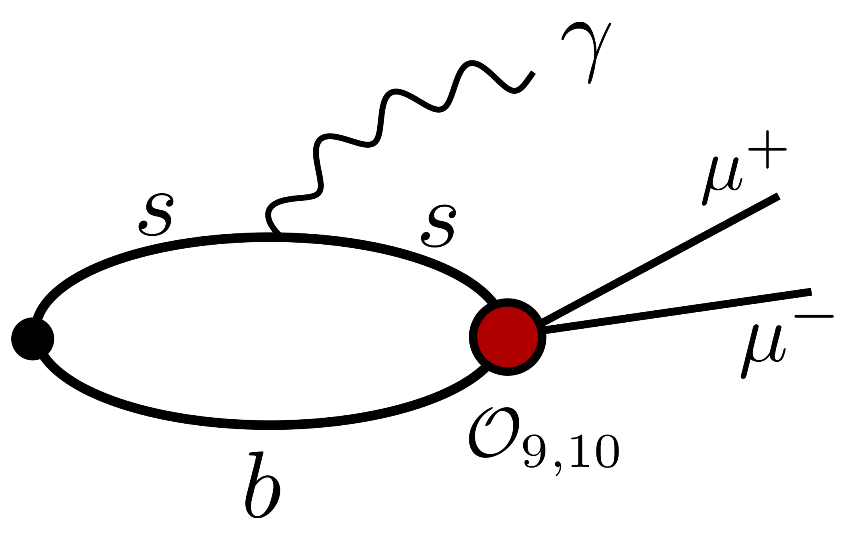


$$H_9^{\mu\nu}(p\,.\,k) = H_{10}^{\mu\nu}(p\,.\,k) = i\int d^4y \langle\, 0\,|\, T\big[\,\bar{s}\,\gamma^\nu\, P_L\, b\,(0)\;\, J^\mu_{\rm em}(y)\big]\;|\,\bar{B}_s(p)\,\rangle$$

$$= -\,i(g^{\mu\nu}\,(k\cdot q) - q^\mu k^\nu)\,\frac{F_A(q^2)}{2m_{B_s}} + \epsilon^{\mu\nu\rho\sigma}\,k_\rho\,q_\sigma\,\frac{F_V(q^2)}{2m_{B_s}}$$

- These form factors can be computed from Euclidean correlation functions (at accessible values of $m_b$).
- We choose $\mathbf{p} = \mathbf{0}$ and $\mathbf{k} = (0,0,k_z)$ and use twisted boundary conditions for $k_z$.
- With such a choice of kinematics: $\frac{1}{2k_z}\left(H_V^{12}(p,k) - H_V^{21}(p,k)\right) \to F_V(x_\gamma)$ and $\frac{i}{2E_\gamma}\left(H_A^{11}(p,k) + H_A^{22}(p,k)\right) \to F_A(x_\gamma)$ .

# The form factors $F_{TV}$ and $F_{TA}$

- In a similar way the following contributions can be computed:

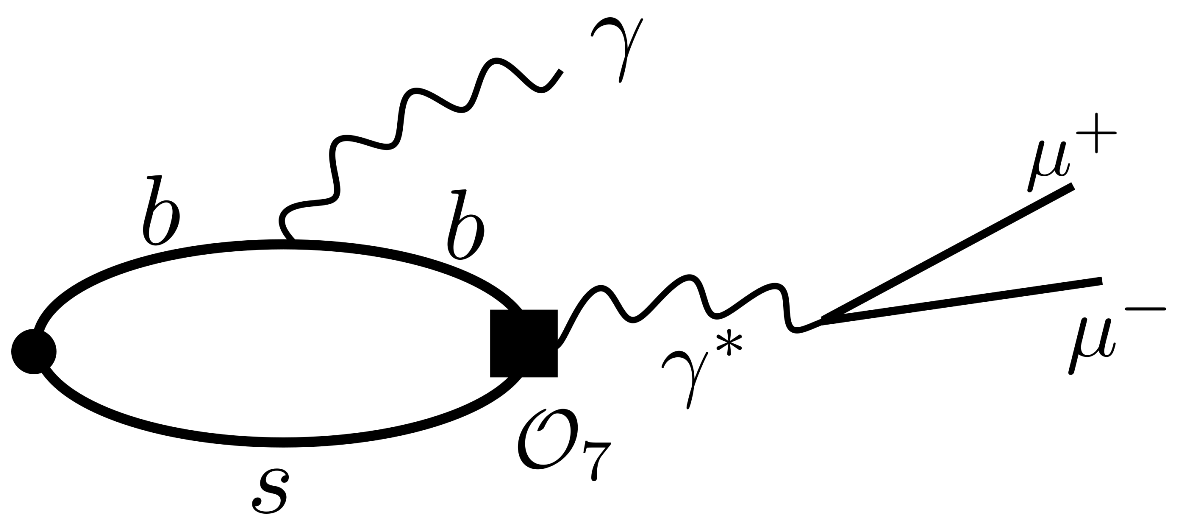


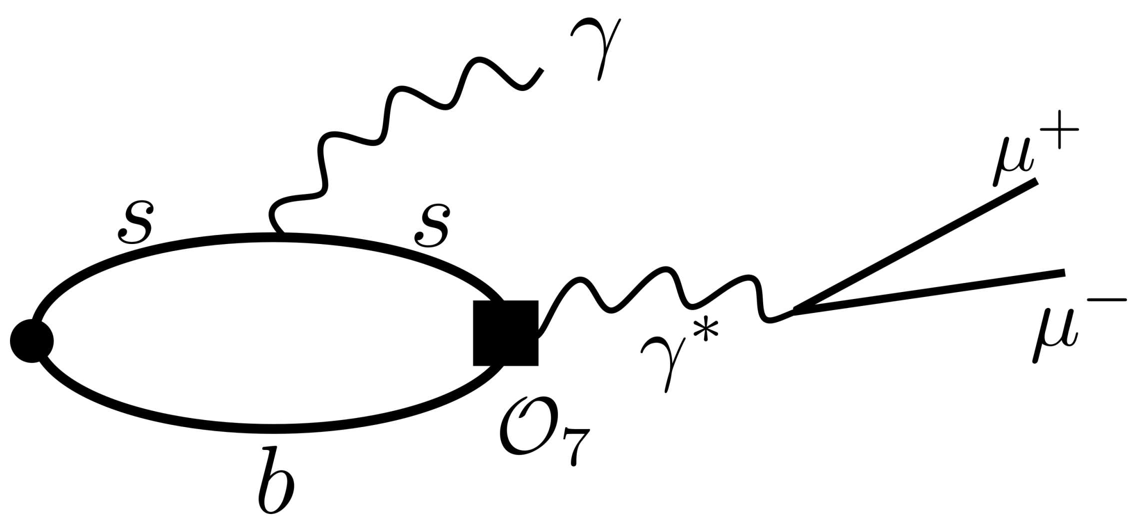


$$H_{7A}^{\mu\nu}(p\,.\,k) = \frac{2m_b}{q^2}\int d^4y\langle\, 0\,|\,T\big[\,\bar{s}\,\sigma^{\nu\rho}\,P_R\,b\,(0)\;J^{\mu}_{\rm em}(y)\big]\,|\,\bar{B}_s(p)\,\rangle$$

$$= -\,i(g^{\mu\nu}\,(k\cdot q) - q^{\mu}k^{\nu})\,\frac{m_bF_{TA}(q^2)}{q^2} + \epsilon^{\mu\nu\rho\sigma}\,k_\rho\,q_\sigma\,\frac{m_bF_{TV}(q^2)}{q^2}$$

- Here, for now, we are isolating the contribution in which it is the virtual photon which is emitted from $O_7$.

- With our choice of kinematics: $\frac{1}{2k_z}\left(H^{12}_{TV}(p,k) - H^{21}_{TV}(p,k)\right) \to F_{TV}(x_\gamma)$ and $\frac{-i}{2E_\gamma}\left(H^{11}_{A}(p,k) + H^{22}_{A}(p,k)\right) \to F_{TA}(x_\gamma)$.

- There is also the useful kinematical constraint that $F_{TV}(1) = F_{TA}(1)$.

# Numerical Results for $F_V$ , $F_A$ , $F_{TV}$ , $F_{TA}$

- These four form-factors can be computed using "standard" methods at the available heavy quark masses.
- We use gauge field configurations generated by the European Twisted Mass Collaboration (ETMC), with the Iwasaki gluon action and $N_f = 2 + 1 + 1$ flavours of Wilson-Clover light quarks at maximal twist (four ensembles with $0.057\ \text{fm} < a < 0.091\ \text{fm}$).
- We perform the calculations at 5 values of the heavy quark mass corresponding to

$$\frac{m_h}{m_c} = 1, 1.5, 2, 2.5 \ \text{and} \ 3\,,$$

  and at 4 values of $x_\gamma = 0.1,\ 0.2,\ 0.3,\ 0.4.$
- $m_c$ is determined from $m_{\eta_c} = 2.984(4)\,\text{GeV}.$
- Much effort is then devoted to the $m_h \to m_b$ and $a \to 0$ limit, guided by the heavy-quark scaling laws and models for possible resonant contributions.

# Continuum Extrapolation

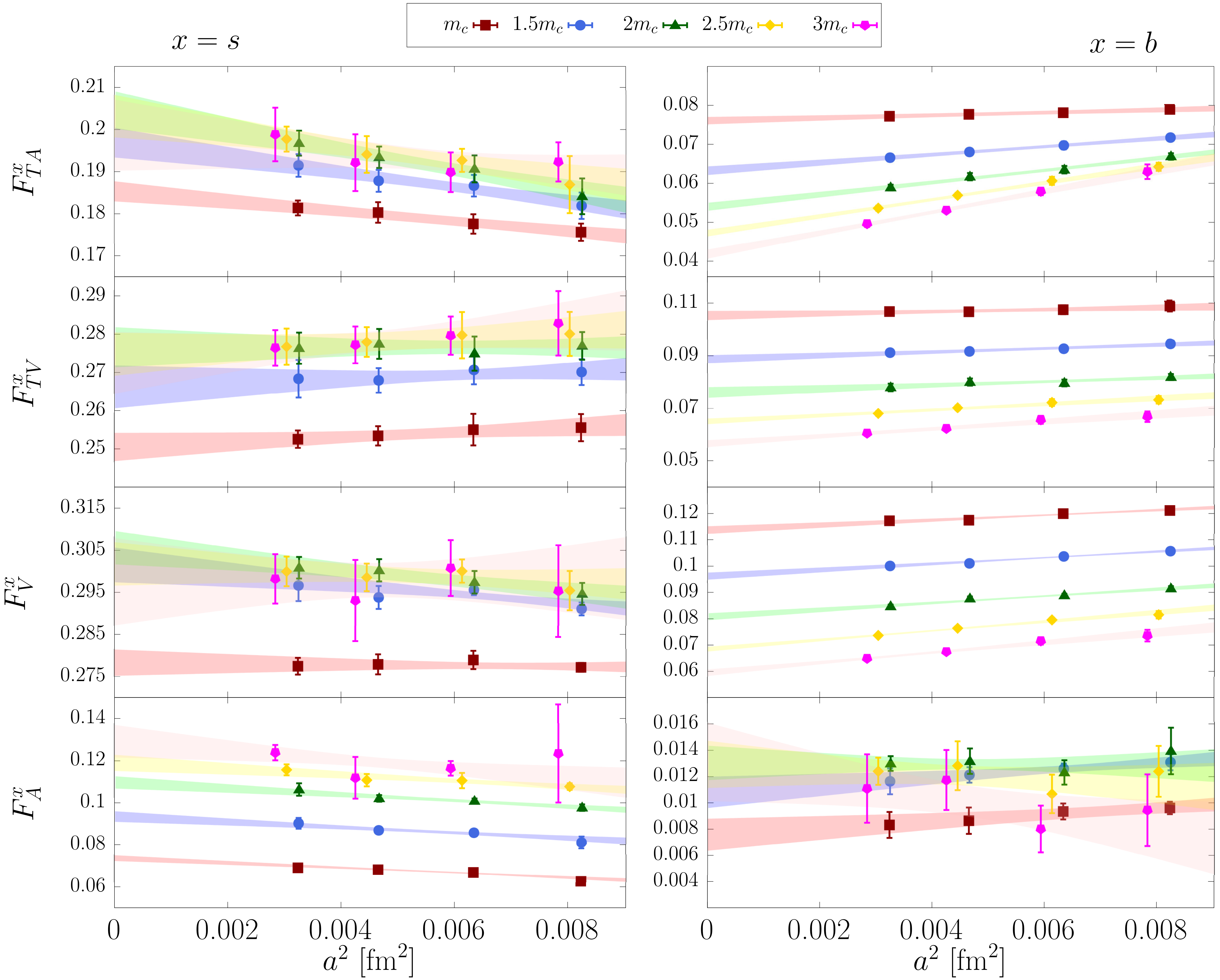


- The continuum extrapolation is performed separately at each value of $m_{H_s}$ and $x_\gamma$ .

- The illustration plots are for $x_\gamma = 0.4$ .

# Extrapolation of the results to $m_{B_s} = 5.367$ GeV

- Having performed the continuum extrapolation, we need to extrapolate the results to the physical value of $m_{B_s}$.
- In the heavy-quark and large $E_\gamma$ limits, scaling laws were derived up to $O(1/m_{H_s}, 1/E_\gamma)$:

M.Beneke and J.Rohrwild, arXiv:1110.3228; M. Beneke, C. Bobeth and Y.-M. Wang, arXiv:2008.12494

$$\frac{F_{V/A}}{f_{H_s}} = \frac{|q_s|}{x_\gamma}\left(\frac{R(E_\gamma,\mu)}{\lambda_B(\mu)} + \xi(x_\gamma, m_{H_s}) \pm \frac{1}{m_{H_s}x_\gamma} \pm \frac{|q_b|}{|q_s|}\frac{1}{m_h}\right) \;;\; \frac{F_{TV/TA}}{f_{H_s}} = \frac{|q_s|}{x_\gamma}\left(\frac{R_T(E_\gamma,\mu)}{\lambda_B(\mu)} + \xi(x_\gamma, m_{H_s}) \pm \frac{1-x_\gamma}{m_{H_s}x_\gamma} + \frac{|q_b|}{|q_s|}\frac{1}{m_{H_s}}\right)$$

- $R(E_\gamma,\mu)$, $R_T(E_\gamma,\mu)$ are radiative correction factors $= 1 + O(\alpha_s)$; $\lambda_B$ is the first inverse moment of the $B_s$-meson LCDA, $\xi(x_\gamma, m_{H_s})$ are power corrections.
- Photon emission from the $b$-quark suppressed relative to the emission from the $s$-quark.
- Tensor form-factors are presented in the $\overline{\text{MS}}$ scheme at $\mu = 5$ GeV.
- However, useful though these scaling laws are, they apply at large $E_\gamma$ (as well as large $m_h$), are there are significant corrections at our lightest values of $m_h$ and smaller values of $E_\gamma$. We therefore us an ansatz which includes the above scaling laws at large $E_\gamma$ as well as VDM behaviour.

# Extrapolation of the results to $m_{B_s} = 5.367$ GeV

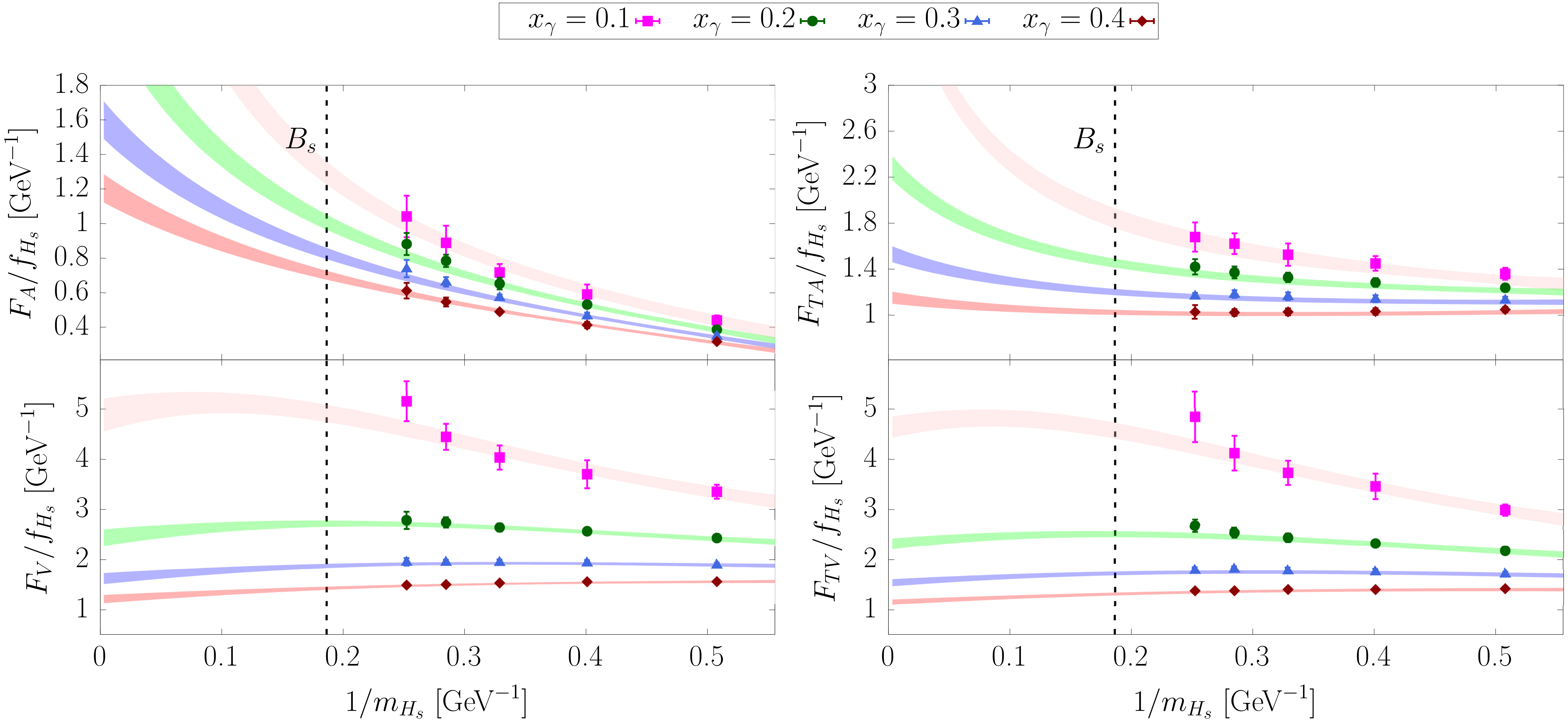

# Comparison with Previous Determinations of the Form Factors

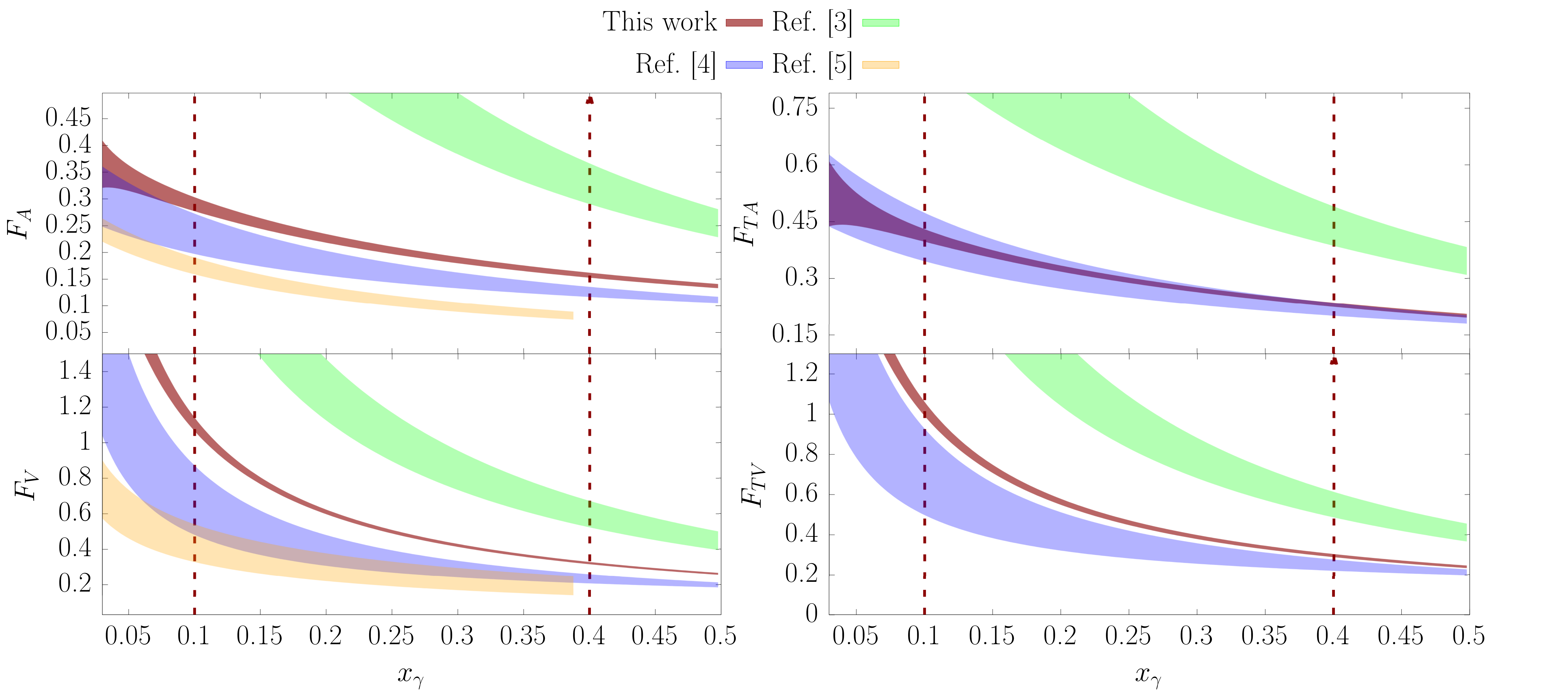


- Ref.[3] = T.Janowski, B.Pullin and R.Zwicky, arXiv:2106.13616, LCSR
- Ref.[4]= A.Kozachuk, D.Melikhov and N.Nikitin, arXiv:1712.07926, relativistic dispersion relations
- Ref.[5]= D.Guadagnoli, C.Normand, S.Simula and L.Vittorio, arXiv:2303.02174, VMD+quark model+lattice at charm

- In general our results for the form factors differ significantly from earlier estimates.

# Other Contributions - $\bar{\mathrm{F}}_{\mathrm{T}}$


$$H^{\mu\nu}_{\bar{T}}(p,k) = i\int d^4y\; e^{i(p-k)\cdot y}\,\langle\, 0\,|\,T\Big[J^{\nu}_{\bar{T}}(0)\;J^{\mu}_{\rm em}(y)\Big]\,|\,\bar{B}_s(\mathbf{0})\,\rangle \equiv -\,\epsilon^{\mu\nu\rho\sigma}\,k_\rho\,p_\sigma \frac{\bar{F}_T}{m_{b_s}} \;\text{ where}$$

$$J^{\nu}_{\bar{T}} = -\,i\,Z_T(\mu)\;\bar{s}\sigma^{\nu\rho}b\;\frac{k^\rho}{m_{B_s}}\;.$$

- The difficulty arises from the first diagram above when $t_y > 0$.
- In that case we potentially have a hadronic intermediate state (e.g. an $s\bar{s}\;\,1^-$ state) with smaller mass than $\sqrt{(p-k)^2}$, leading to an imaginary part and problems with the continuation to Euclidean space.

$$\sqrt{m_V^2+E_\gamma^2}+E_\gamma < m_{B_s} \;\Rightarrow\; x_\gamma < 1-\frac{m_V^2}{m_{B_s}^2} \simeq 1-\frac{4m_K^2}{m_{B_s}^2} \simeq 0.96\,.$$

# $\bar{\mathbf{F}}_\mathbf{T}$ (cont.)

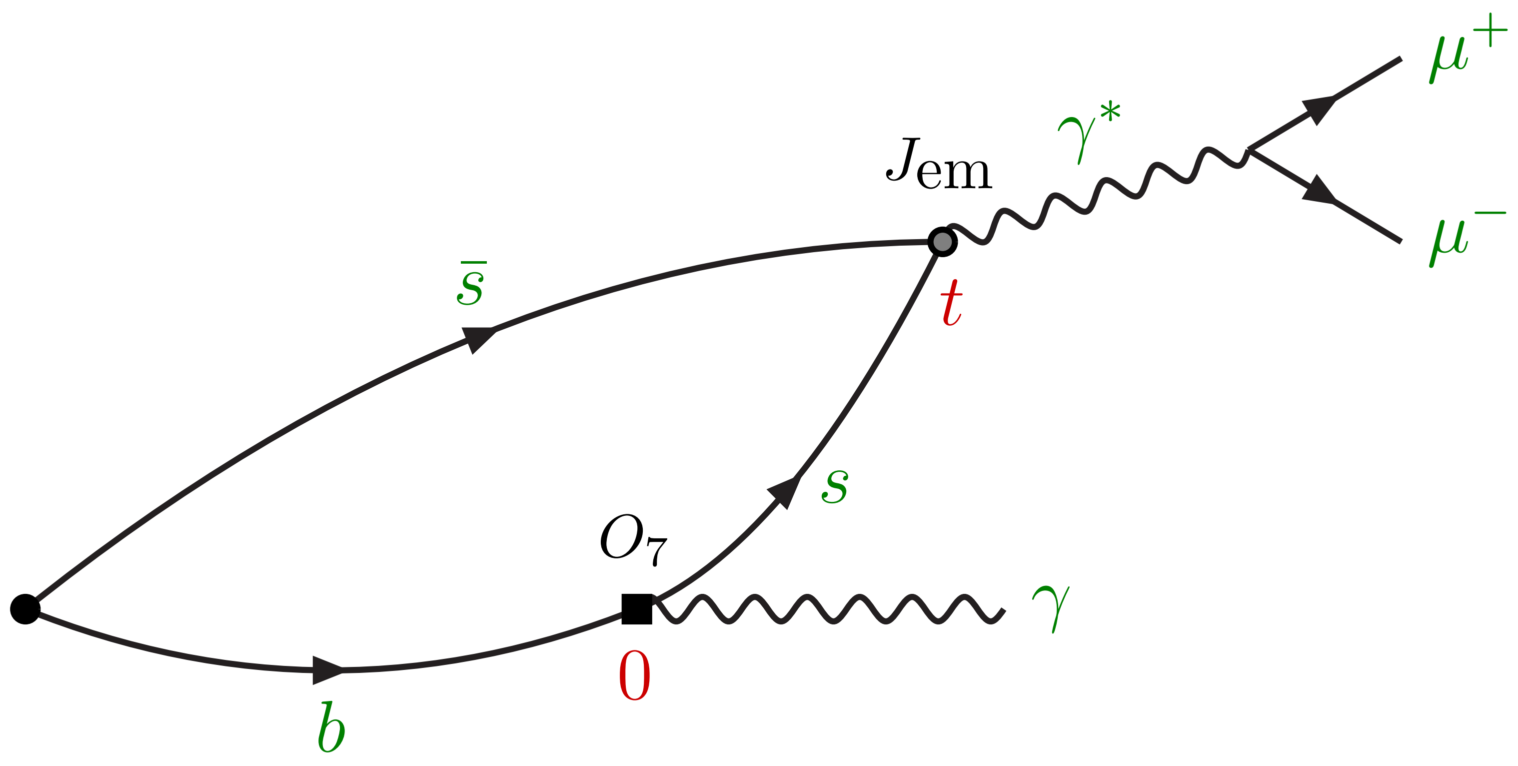


- Large amount of effort is being devoted to developing techniques based on the spectral density representation,

M.Hansen, A.Lupo and N.Tantalo, arXiv:1903.06476
R.Frezzotti et al., arXiv:2306.07228

- For $t > 0$ define $C_s(t, \mathbf{k}) = \langle\, 0\,|\, J^\mu_{{\rm em},s}(t, -\mathbf{k})\, J^\nu_{\bar{T}}(0)\,|\, B_s(\mathbf{0})\rangle \;=\; \displaystyle\int_{-\infty}^{\infty} dt'\,\delta(t'-t)\, C_s(t', -\mathbf{k})$

$$= \int_{-\infty}^{\infty} dt' \int_{-\infty}^{\infty} \frac{dE'}{2\pi}\, e^{iE'(t'-t)}\, C_s(t', -\mathbf{k}) = \int_{-\infty}^{\infty} \frac{dE'}{2\pi}\, e^{-iE't} \int d^4x'\, e^{ik'\cdot x'}\, \langle 0\,|\, J^\mu_{{\rm em},s}(x')\, J^\nu_{\bar{T}}(0)\,|\, B(\mathbf{0})\rangle \qquad \big(k' = (E', -\mathbf{k})\big)$$

$$= \int_{-\infty}^{\infty} \frac{dE'}{2\pi}\, e^{-iE't} \int d^4x'\, \langle 0\,|\, J^\mu_{{\rm em},s}(0)\, e^{-i(\hat{P}-k')\cdot x'}\, J_{\bar{T}}T^\nu(0)\,|\, B(\mathbf{0})\rangle = \int_{-\infty}^{\infty} \frac{dE'}{2\pi}\, e^{-iE't}\, \underbrace{\langle 0\,|\, J^\mu_{{\rm em},s}(0)\, (2\pi)^4\, \delta(\hat{P}-k')\, J^\nu_{\bar{T}}(0)\,|\, B(\mathbf{0})\rangle}_{\rho_s(E', \mathbf{k})}$$

$$\equiv \int_{-\infty}^{\infty} \frac{dE'}{2\pi}\, e^{-iE't}\, \rho_s^{\mu\nu}(E', \mathbf{k})$$

- In Euclidean space $C_s(t, \mathbf{k}) = \displaystyle\int_{E^*}^{\infty} \frac{dE'}{2\pi}\, e^{-E't}\, \rho_s^{\mu\nu}(E', \mathbf{k})\,.$

# $\bar{\mathbf{F}}_{\mathbf{T}}$ (cont.)

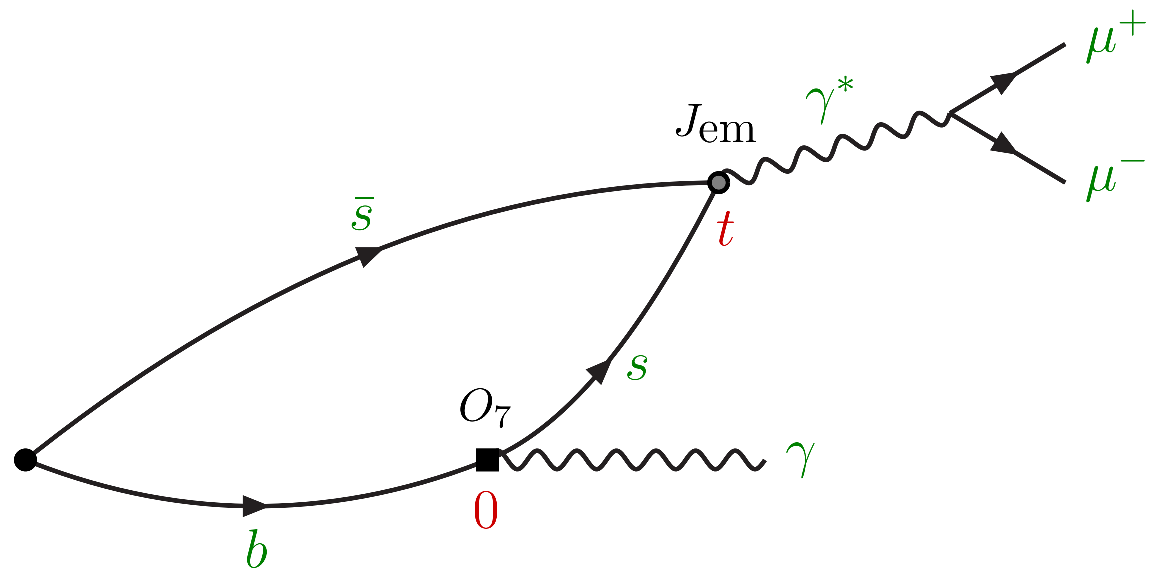


- For $t > 0$ define $C_s(t, \mathbf{k}) = \langle 0 \,|\, J^{\mu}_{\mathrm{em},s}(t, -\mathbf{k})\, J^{\nu}_{T}(0) \,|\, B_s(\mathbf{0}) \rangle \;=\; \int_{E^*}^{\infty} \frac{dE'}{2\pi}\, e^{-iE't}\, \rho_s^{\mu\nu}(E', k)\,.$
- In Euclidean space $C_s(t, \mathbf{k}) \;=\; \int_{E^*}^{\infty} \frac{dE'}{2\pi}\, e^{-E't}\, \rho_s^{\mu\nu}(E', k)\,.$

- For the amplitude we require

$$H^{\mu\nu}_{\bar{T}_s}(m_B, \mathbf{k}) \;=\; i \int_0^{\infty} dt\; e^{i(m_B-\omega)t}\, C_s^{\mu\nu}(t, \mathbf{k}) \;=\; \lim_{\epsilon\to 0} \int_{E^*}^{\infty} \frac{dE'}{2\pi}\, \frac{\rho_s^{\mu\nu}(E', \mathbf{k})}{E' - (m_B - \omega) - i\epsilon}\,. \qquad \big(\omega = |\,\mathbf{k}\,|\,\big)$$

- The question is how (best) to extract the information about the spectral density, $\rho_s^{\mu\nu}(E, k)$, contained in the Euclidean correlation function in order to determine the amplitude (both the real and imaginary parts).

- We use the HLT method, in which computations are performed at several values of $\epsilon$, and the kernel $\dfrac{1}{E' - (m_B - \omega) - i\epsilon}$ is approximated by a series of exponentials in time.

$$\frac{1}{E' - E - i\epsilon} \simeq \sum_{n=1}^{n_{\max}} g_n(E, \epsilon)\, e^{-anE'} \qquad \text{where the } g_n \text{ are complex coefficients.}$$

- Finally $H^{\mu\nu}_{\bar{T}_s}(m_B, \mathbf{k}) \;=\; \lim_{\epsilon\to 0} \int_{E^*}^{\infty} \frac{dE'}{2\pi}\, \frac{\rho_s^{\mu\nu}(E', \mathbf{k})}{E' - (m_B - \omega) - i\epsilon} \;=\; \lim_{\epsilon\to 0} \sum_{n=1}^{n_{\max}} g_n(m_B - \omega, \epsilon)\, C_s(an, \mathbf{k})$

# $\bar{\mathbf{F}}_{\mathbf{T}}$ (cont.)

- Determining the $g_n$ requires a balance between the systematic error due to the approximation of $1/(E' - E - i\epsilon)$ by a finite number of exponentials (in which the coefficients are large with alternating signs) and the statistical errors in the correlation functions $C_s(an, \mathbf{k})$.

- We have computed $\bar{F}_T$ at all four values of $x_\gamma$, at three of the five values of $m_h$ $(m_h/m_c = 1, 1.5, 2.5)$ and on two of the gauge-field ensembles ($a = 0.0796(1)$ fm and $0.0569(1)$ fm).
    i) $\bar{F}_T$ only gives a very small contribution to the rate and is therefore not needed with great precision.
    ii) The spectral density method is computationally expensive.

- An extrapolation in $\epsilon$ is required, as well as those in $a$ and $m_h$ .

- Resulting error is $O(100\%)$ but $\bar{F}_T \ll F_{TV}, F_{TA}$ . No clear $x_\gamma$ dependence is observed in our data and we quote:

$$\mathrm{Re}\,\bar{F}_T^s(x_\gamma) = -0.019(19) \;\text{ and }\; \mathrm{Im}\,\bar{F}_T^s(x_\gamma) = 0.018(18)\,.$$

# $\bar{F}^s_T$ - Illustrative Plots

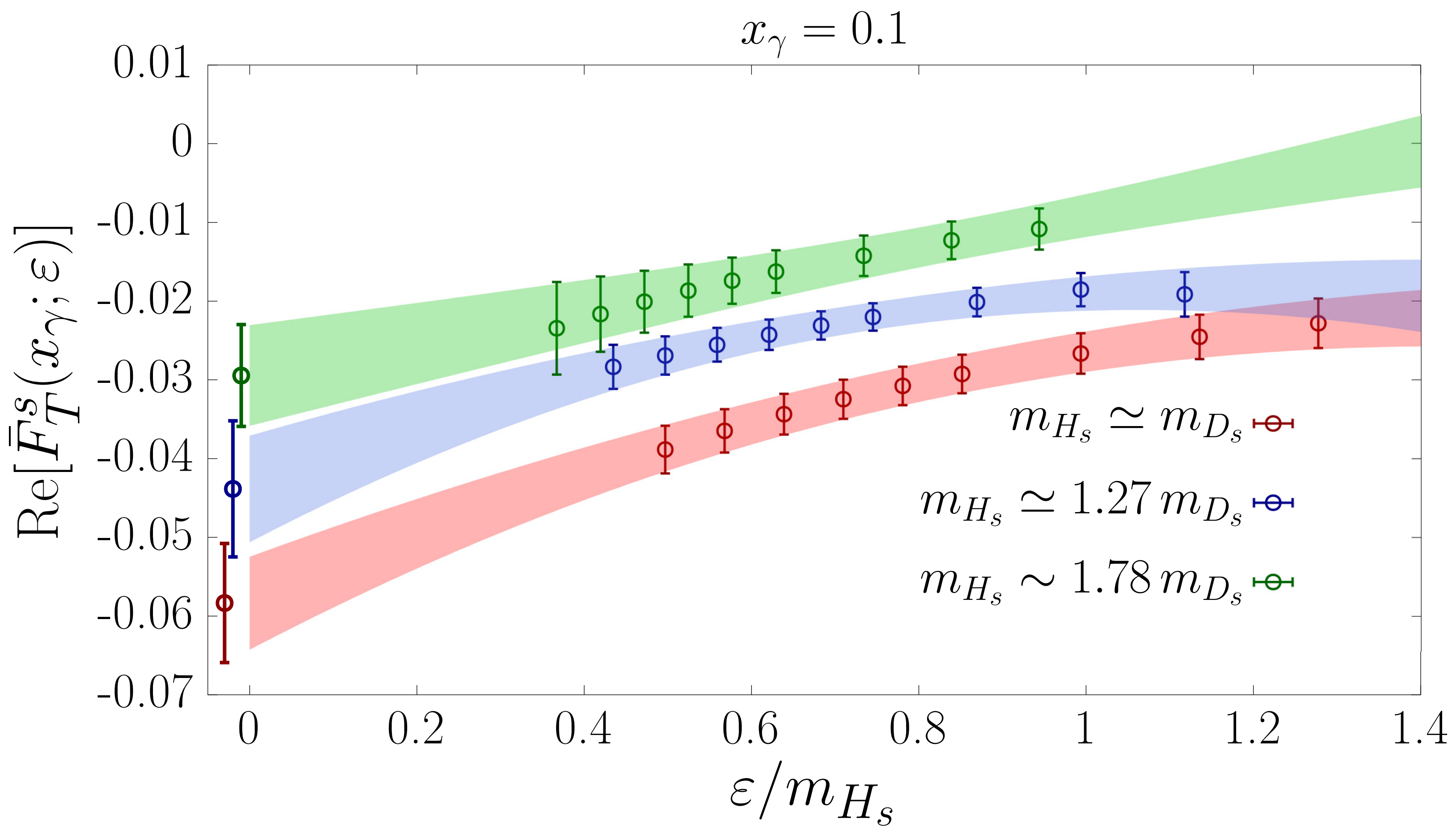


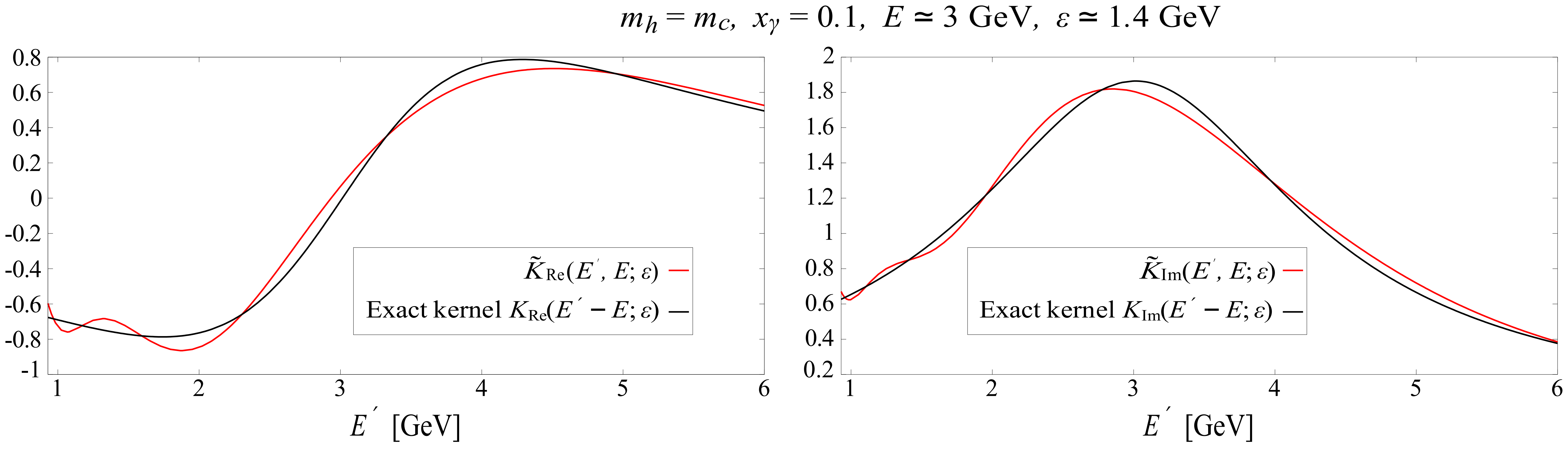


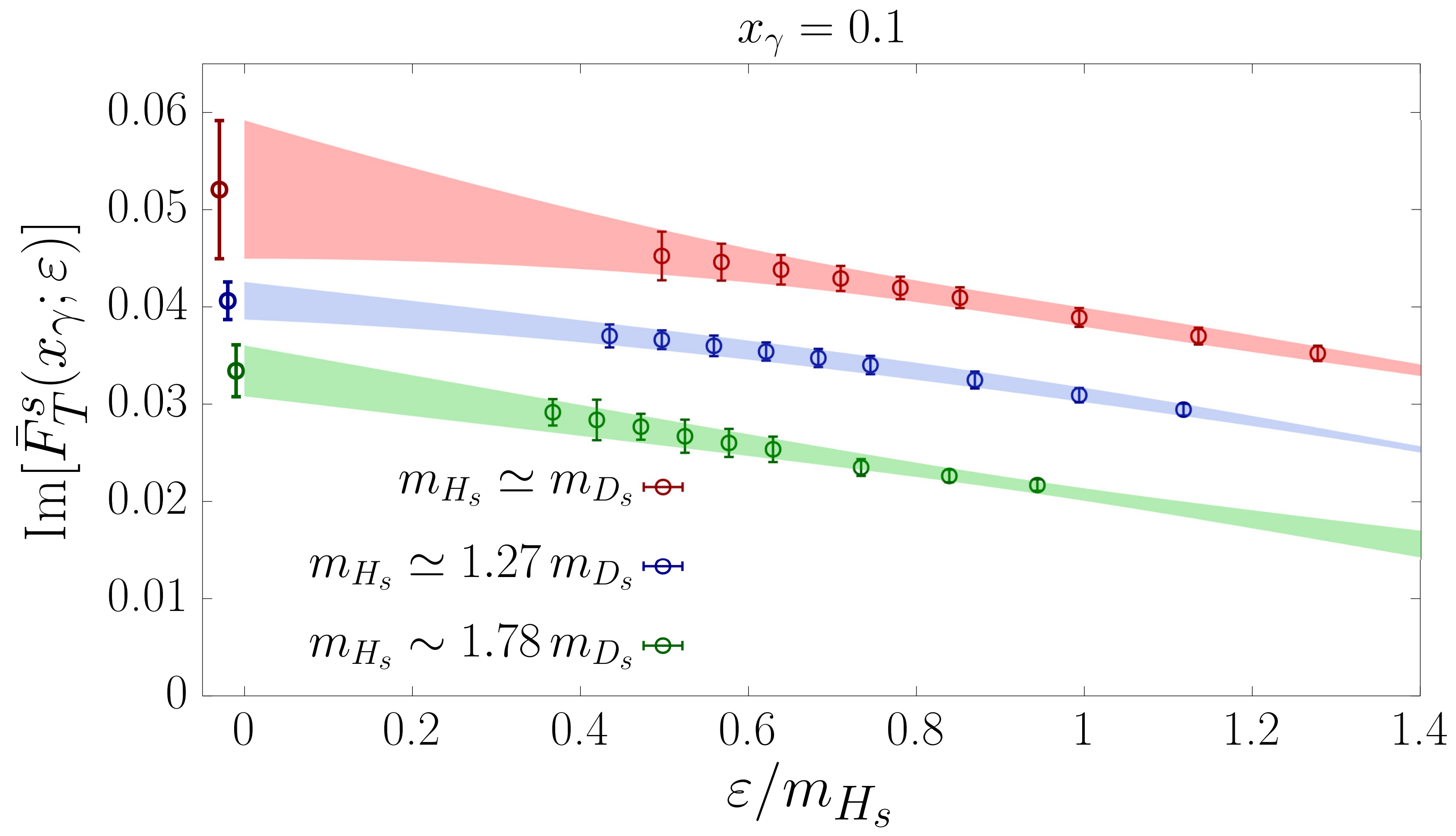


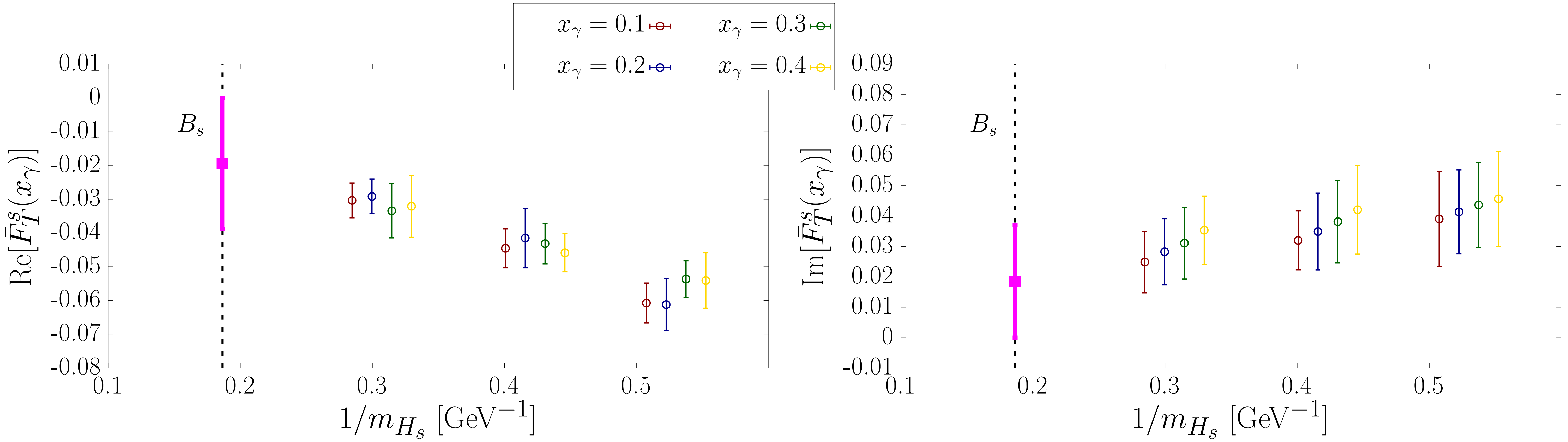

# Other Contributions - Charming Penguins

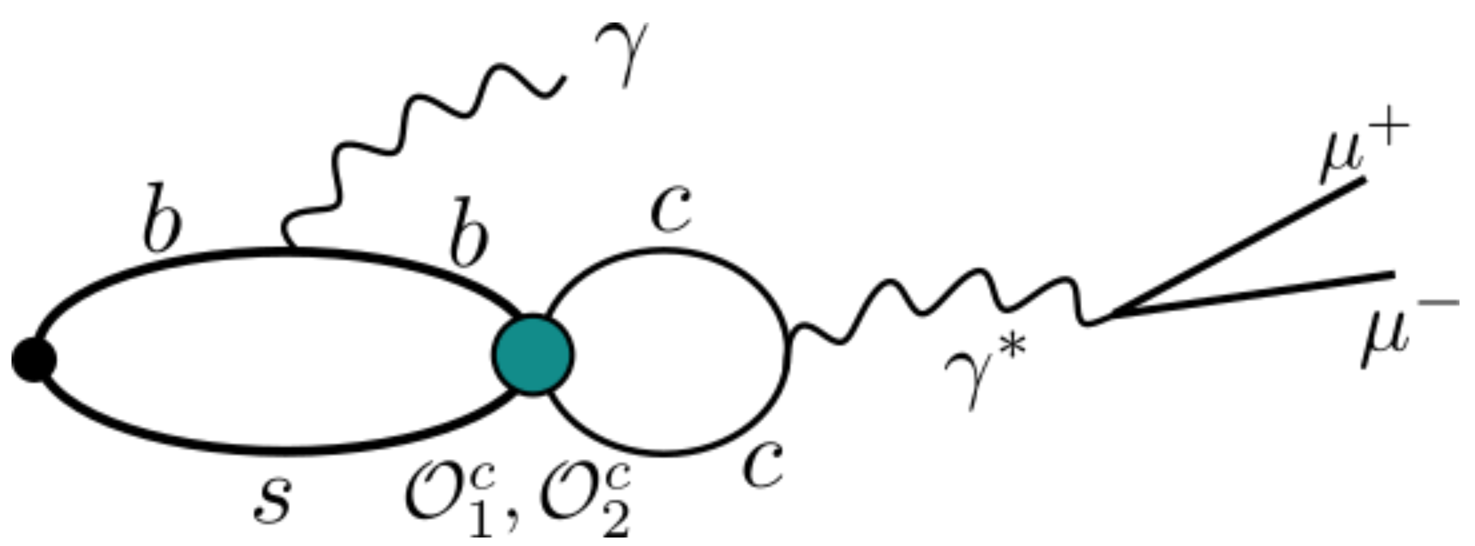


- Of the contributions we have not computed directly , the most significant one at large $q^2$ is expected to be that from the operators $O^c_{1,2}$ (charming penguins) and we are working on developing methods to overcome this. There are a number of new theoretical issues to be understood.

- In the meantime we follow previous ideas and estimate the contribution based on VMD inserting all $c\bar{c}$ resonances from the $J/\Psi$ to the $\Psi(4660)$ . It can be viewed as a shift in $C_9 \to C_9^{\text{eff}}(q^2) = C_9 + \Delta C_9(q^2)$ :

$$\Delta C_9(q^2) = -\frac{9\pi}{\alpha_{\text{em}}^2}\left(C_1 + \frac{C_2}{3}\right)\sum_V |k_V| e^{i\delta_V} \frac{m_V\Gamma_V\, B(V \to \mu^+\mu^-)}{q^2 - m_V^2 + i m_V \Gamma_V}\,.$$

- $k_V$ and $\delta_V$ parametrise the deviation from the factorisation approximation (in which $\delta_V = k_V - 1 = 0$). We allow $\delta_V$ to vary over $(0,2\pi)$ and $|k_V|$ to vary in the range $1.75 \pm 0.75$ .

# Branching Fractions

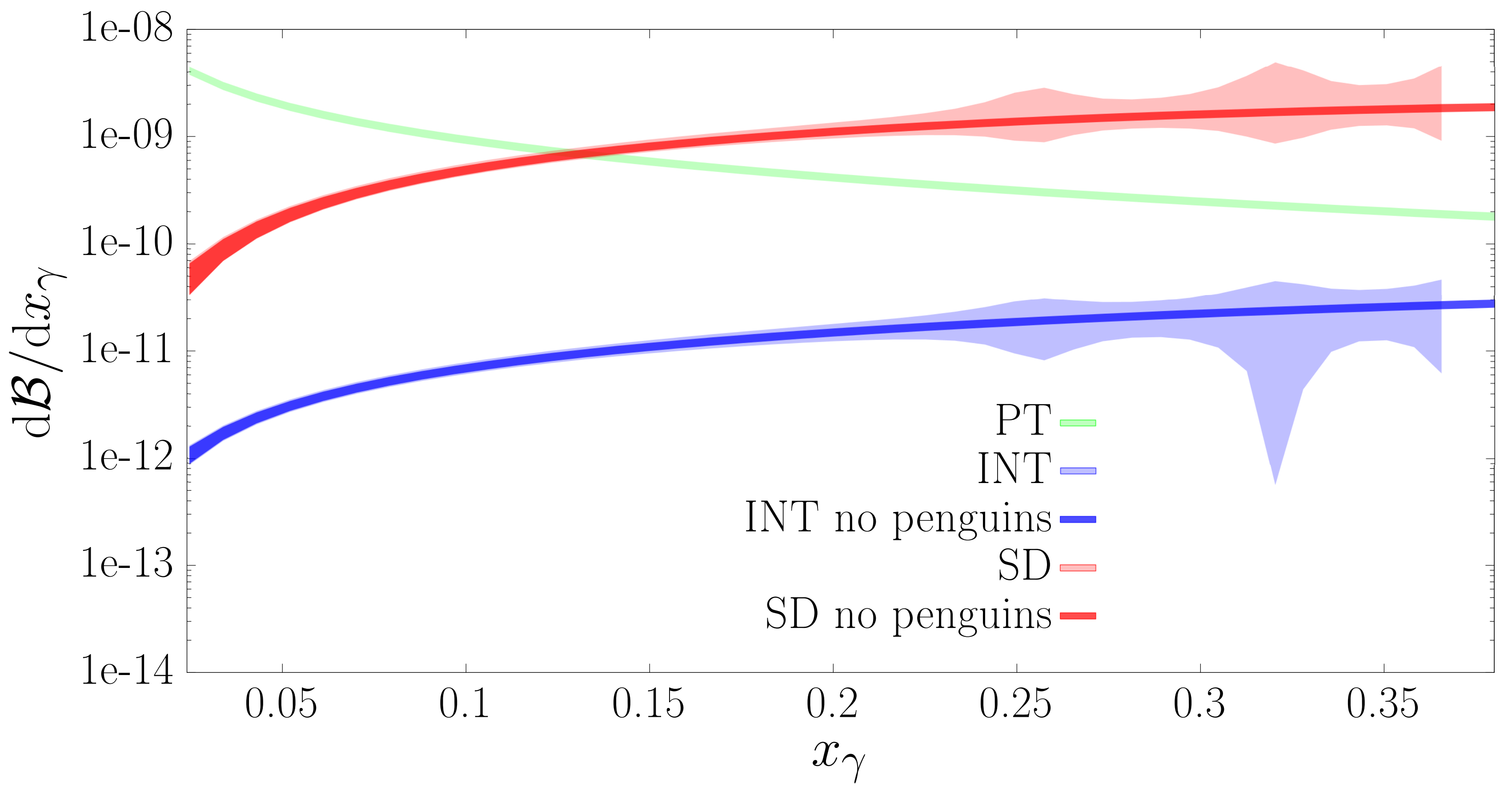


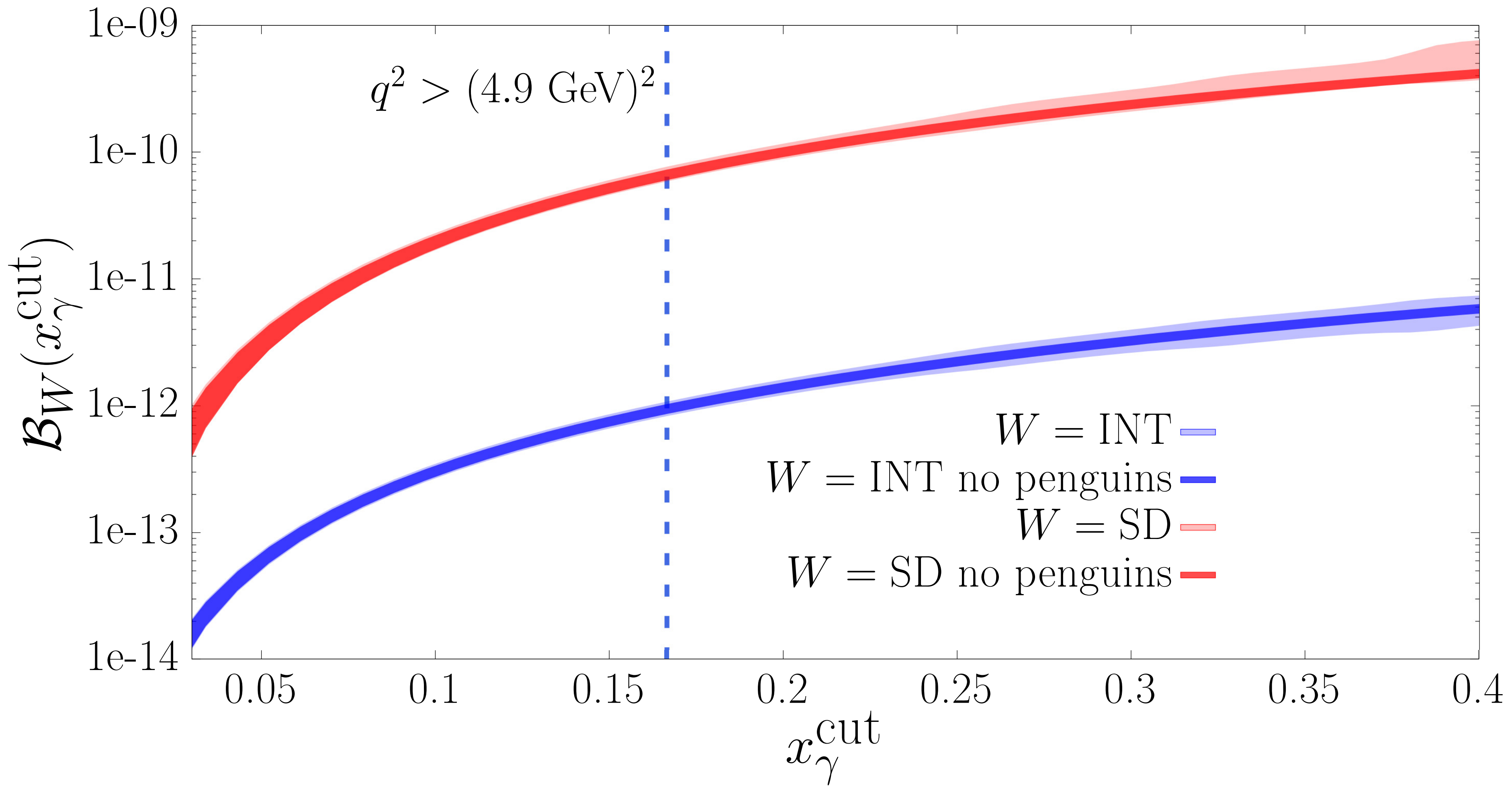


$$\mathscr{B}(x_\gamma^{\rm cut}) = \int_0^{x_\gamma^{\rm cut}} dx_\gamma \, \frac{d\mathscr{B}(x_\gamma)}{dx_\gamma}$$

- Structure Dependent (SD) contribution dominated by $F_V$.
- The error from the charming penguins increases with $x_\gamma$ (at $x_\gamma = 0.4$ it is about $30\,\%$ ).
- Our Result - $\mathscr{B}_{\rm SD}(0.166) = 6.9(9) \times 10^{-11}$; LHCb - $\mathscr{B}_{\rm SD}(0.166) < 2 \times 10^{-9}$.

# Comparisons

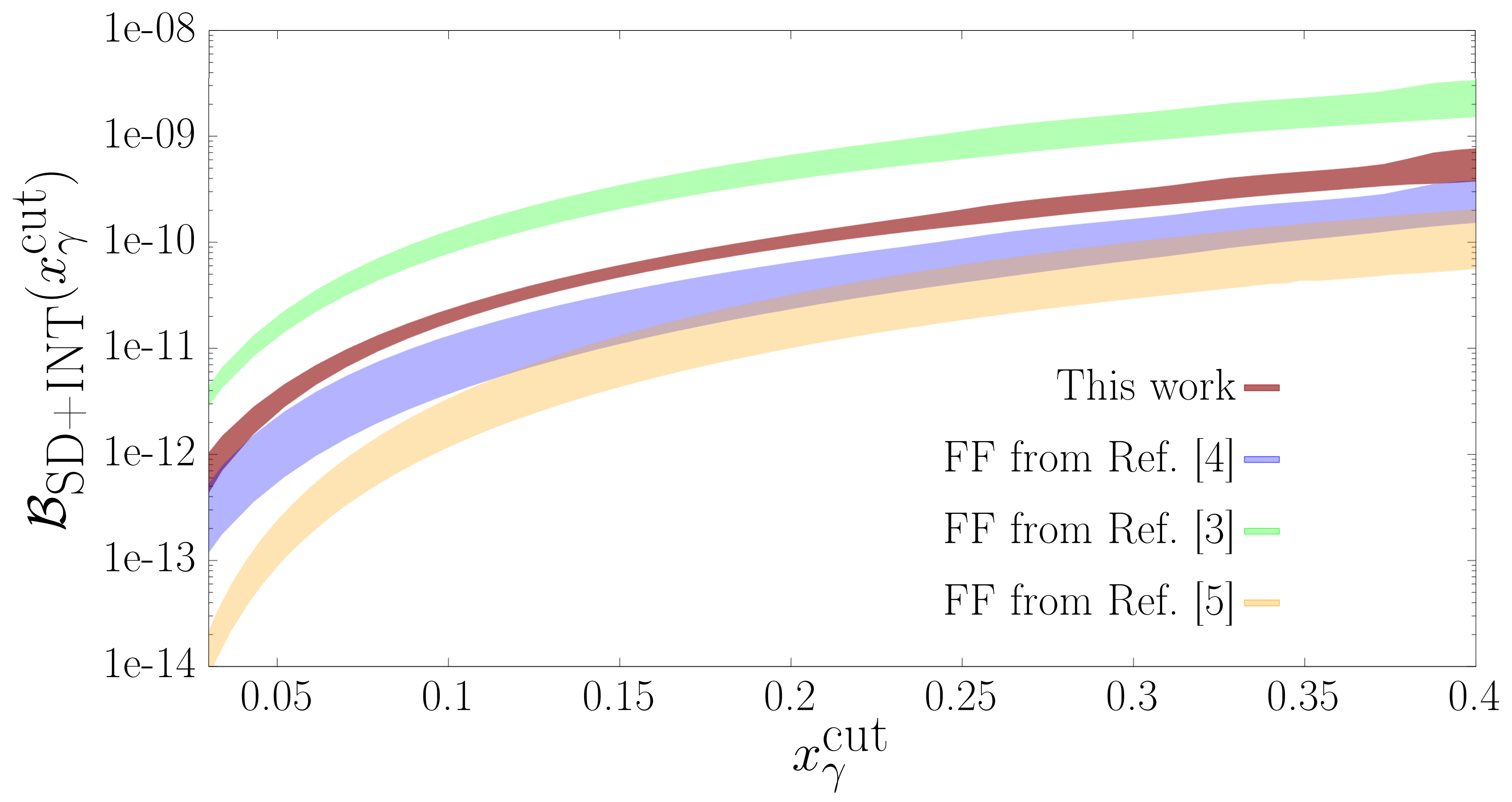


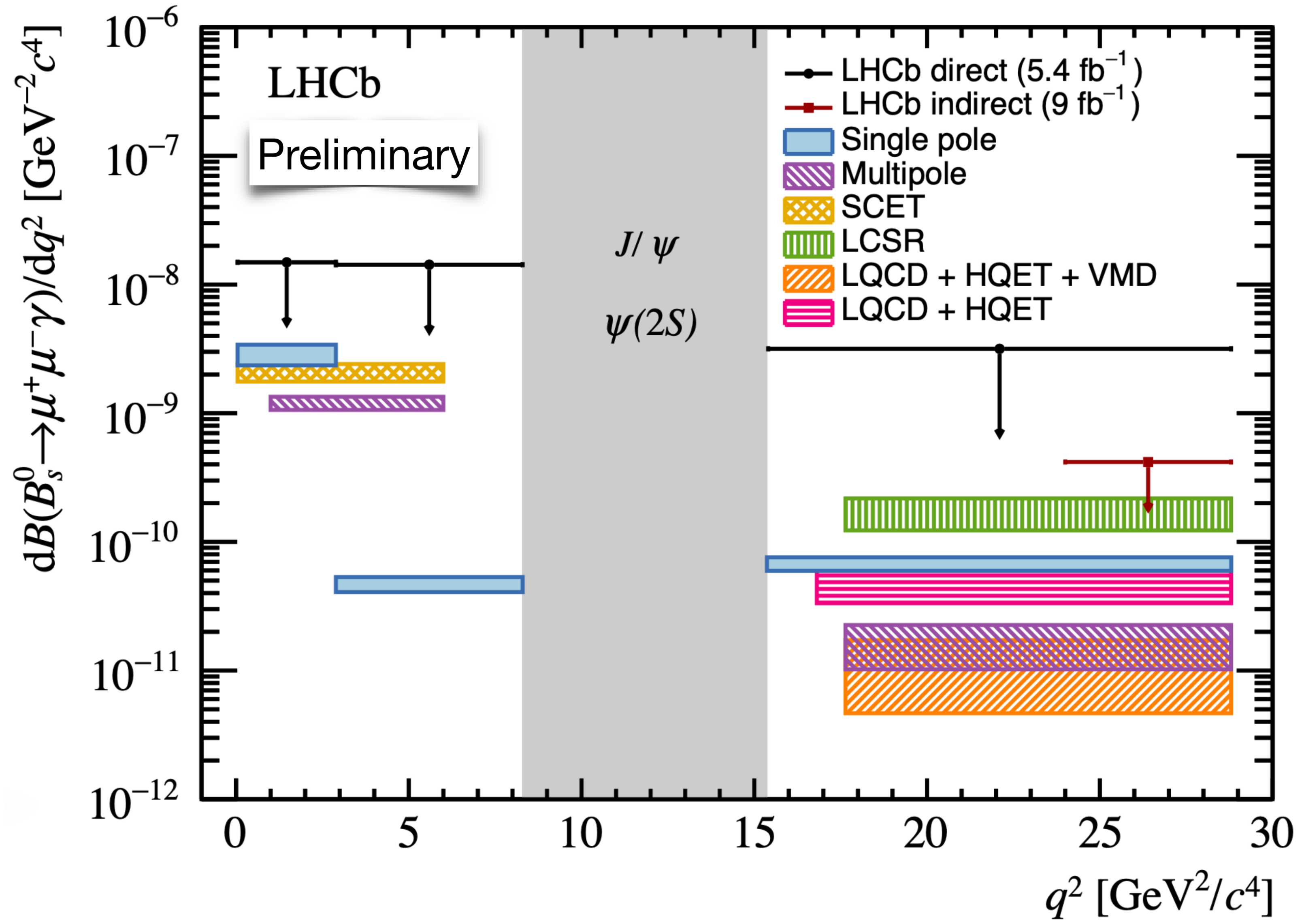


- Ref.[3] = T.Janowski, B.Pullin and R.Zwicky, arXiv:2106.13616, LCSR
- Ref.[4]= A.Kozachuk, D.Melikhov and N.Nikitin, arXiv:1712.07926, relativistic dispersion relations
- Ref.[5]= D.Guadagnoli, C.Normand, S.Simula and L.Vittorio, arXiv:2303.02174, VMD+quark model+lattice at charm
- Discrepancy persists since rate dominated by $F_V$

- New LHCb update with direct detection of final state photon.

I.Bachiller, La Thuile 2024
LHCb, 2404.07648

- For $q^2 > 15\,\mathrm{GeV}^2$ the bound is about an order of magnitude higher than before.

# $\bar{B}_s \to \mu^+\mu^-\gamma$ — Conclusions

- We have computed the form factors $F_V$, $F_A$, $F_{TV}$ and $F_{TA}$ which contribute to the amplitude. The amplitude is dominated by $F_V$.
  *There are significant discrepancies with earlier estimates of the form factors obtained using other methods.*

- As $q^2$ is decreased towards the region of charmonium resonances, the uncertainties grow, from 15 % with $\sqrt{q^2_{\rm cut}} = 4.9\,\mathrm{GeV}$ to about 30 % for $\sqrt{q^2_{\rm cut}} = 4.2\,\mathrm{GeV}$, largely due to the charming penguins for which we have included a phenomenological parametrisation.

## Outlook

- Develop methods which would allow the evaluation of the charming penguin contributions, also for $B \to K^{(*)}\mu^+\mu^-$ decays etc.. *This is one of our top priorities!*

- Continue developing methods to evaluate the disconnected diagrams.

- Continue performing simulations on finer lattices so that the uncertainties due to the $m_h \to m_b$ extrapolation are reduced.

# 4. $P \to \ell \bar{\nu}_\ell \ell'^+ \ell'^-$ Decays

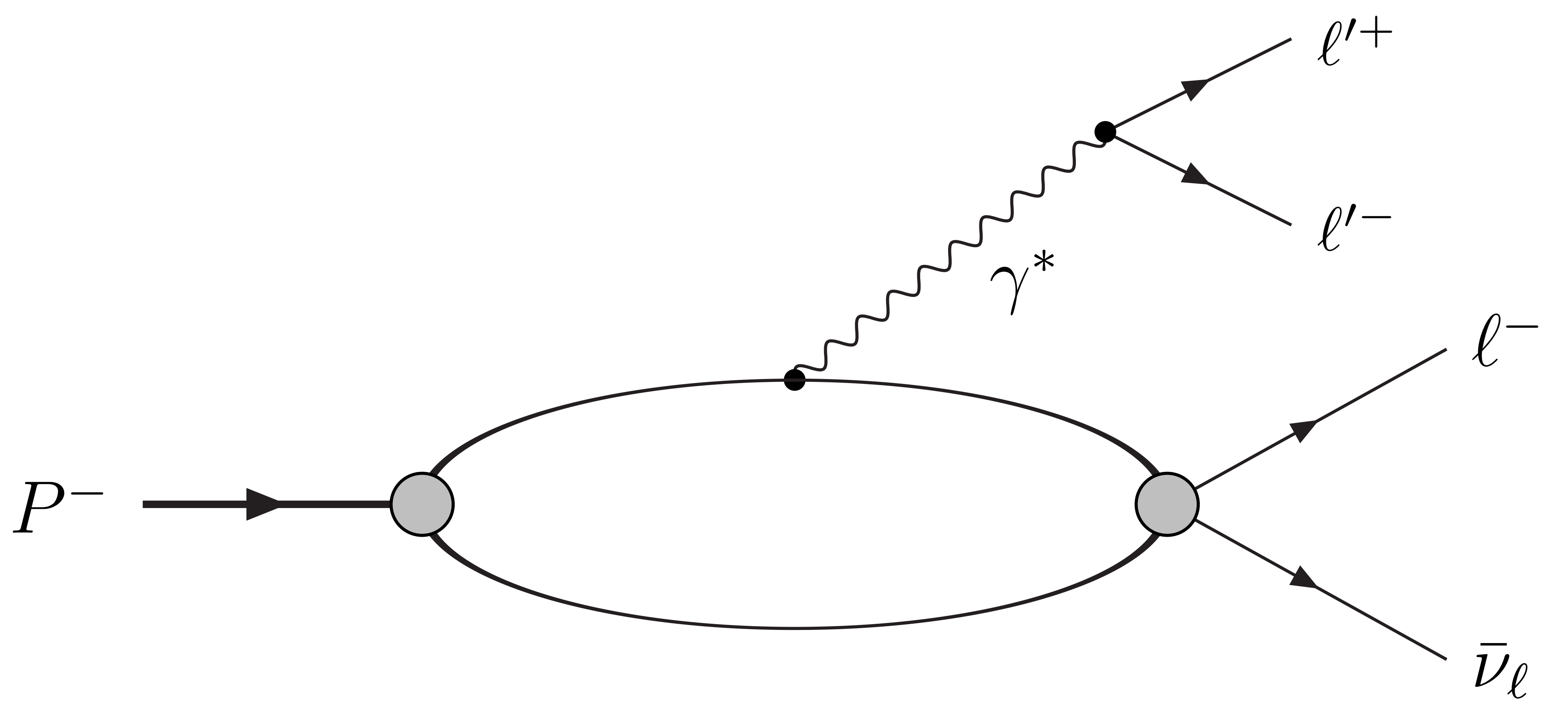


- Non-perturbative contribution to $P \to \ell \bar{\nu}_\ell \gamma$ is encoded in:

$$H_W^{\alpha r}(k, \mathbf{p}) = \epsilon_\mu^r(k)\, H_W^{\alpha\mu}(k, \mathbf{p}) = \epsilon_\mu^r(k) \int d^4y\, e^{ik\cdot y}\, \mathrm{T}\ \langle 0 |\, j_W^\alpha(0)\, j_{\rm em}^\mu(y)\, |\, P(\mathbf{p})\, \rangle$$

$$= \epsilon_\mu^r(k) \left\{ \frac{H_1}{m_K} \left[k^2 g^{\mu\alpha} - k^\mu k^\alpha\right] + \frac{H_2}{m_K} \frac{\left[(p\cdot k - k^2)k^\mu - k^2(p-k)^\mu\right](p-k)^\alpha}{(p-k)^2 - m_K^2} \right.$$

$$\left. -i\frac{F_V}{m_K}\varepsilon^{\mu\alpha\gamma\beta}k_\gamma p_\beta + \frac{F_A}{m_K}\left[(p\cdot k - k^2)g^{\mu\alpha} - (p-k)^\mu k^\alpha\right] + f_P \left[ g^{\mu\alpha} - \frac{(2p-k)^\mu (p-k)^\alpha}{(p-k)^2 - m_K^2} \right] \right\}$$

- Now all four Structure-Dependent form factors have to be determined.

# $\mathrm{P} \to \ell \bar{\nu}_\ell \ell'^+ \ell'^-$ Decays (Cont,)

- We have performed an exploratory calculation with $P = K$ at unphysical quark masses in order to develop a strategy to extract the four form factors and to check whether they can be determined with good precision.

G.Gagliardi et al., arXiv:2202.03833

- The computations were performed on a single ETMC ensemble, with $N_f = 2 + 1 + 1$ dynamical quark flavours, a space-time volume $32^3 \times 64$, $a = 0.0885(36)$ fm and with quark masses such that $m_\pi \simeq 320\,\mathrm{MeV}$ and $m_K \simeq 530\,\mathrm{MeV}$.
    - With $m_K < 2m_\pi$ we have the unphysical simplification that there is no difficulty in the Minkowski → Euclidean continuation.

- There had also been a similar exploratory computation of these decays (calculating the rates without determining the form factors) on a $24^3 \times 48$ lattice, $a \simeq 0.093$ fm, and with quark masses corresponding to $m_\pi \simeq 352\,\mathrm{MeV}$ and $m_K \simeq 506\,\mathrm{MeV}$ .

X.-Y.Tuo, X.Feng, L.-C.Jin and T.Wang, arXiv:2103.11331

# Results from the Exploratory Computations

| Decay | this work | Point-like | Tuo et al. | ChPT($f_\pi$) | ChPT($f_K$) | Experiment |
|---|---|---|---|---|---|---|
| $K^+ \to e^+\nu_e\,\mu^+\mu^-$ | $0.762(49) \times 10^{-8}$ | $3.0 \times 10^{-13}$ | $0.94(8) \times 10^{-8}$ | $1.19 \times 10^{-8}$ | $0.62 \times 10^{-8}$ | $1.72(45) \times 10^{-8}$ |
| $K^+ \to \mu^+\nu_\mu\,e^+e^-$ $x_k > 0.284$ | $8.26(13) \times 10^{-8}$ | $4.8 \times 10^{-8}$ | $11.08(39) \times 10^{-8}$ | $9.82 \times 10^{-8}$ | $8.25 \times 10^{-8}$ | $7.93(33) \times 10^{-8}$ |
| $K^+ \to \mu^+\nu_\mu\,\mu^+\mu^-$ | $1.178(35)\times10^{-8}$ | $3.7 \times 10^{-9}$ | $1.52(7) \times 10^{-8}$ | $1.51(7) \times 10^{-8}$ | $1.10 \times 10^{-8}$ | - |
| $K^+ \to e^+\nu_e\,e^+e^-$ $x_k > 0.284$ | $1.95(11) \times 10^{-8}$ | $2.0 \times 10^{-12}$ | $3.29(35) \times 10^{-8}$ | $3.34 \times 10^{-8}$ | $1.75 \times 10^{-8}$ | $2.91(23) \times 10^{-8}$ |

- $x_k = \sqrt{k^2/m_K^2}$ where $k^2 = (p_{\ell'^+} + p_{\ell'^-})^2$ .
- At NLO ChPT, $F_V = \dfrac{m_K}{4\sqrt{2}\pi^2 F}$, $F_A = \dfrac{4\sqrt{2}m_K}{F}(L_9^r + L_{10}^r)$, $H_1(k^2) = 2f_K m_K \dfrac{F_V(k^2) - 1}{k^2} = H_2(k^2)$ .
- Since the lattice results presented above are at unphysical quark masses, the comparison with the experimental results should not be taken very seriously, nevertheless they are encouraging.

- Experiment = E865 at BNL, HMa et al., hep-ex/0505011 and R.Aaij et al., arXiv:1812.06004

# $K \to \ell \bar{\nu}_\ell \ell'^+ \ell'^-$ Decays — Status and Prospects

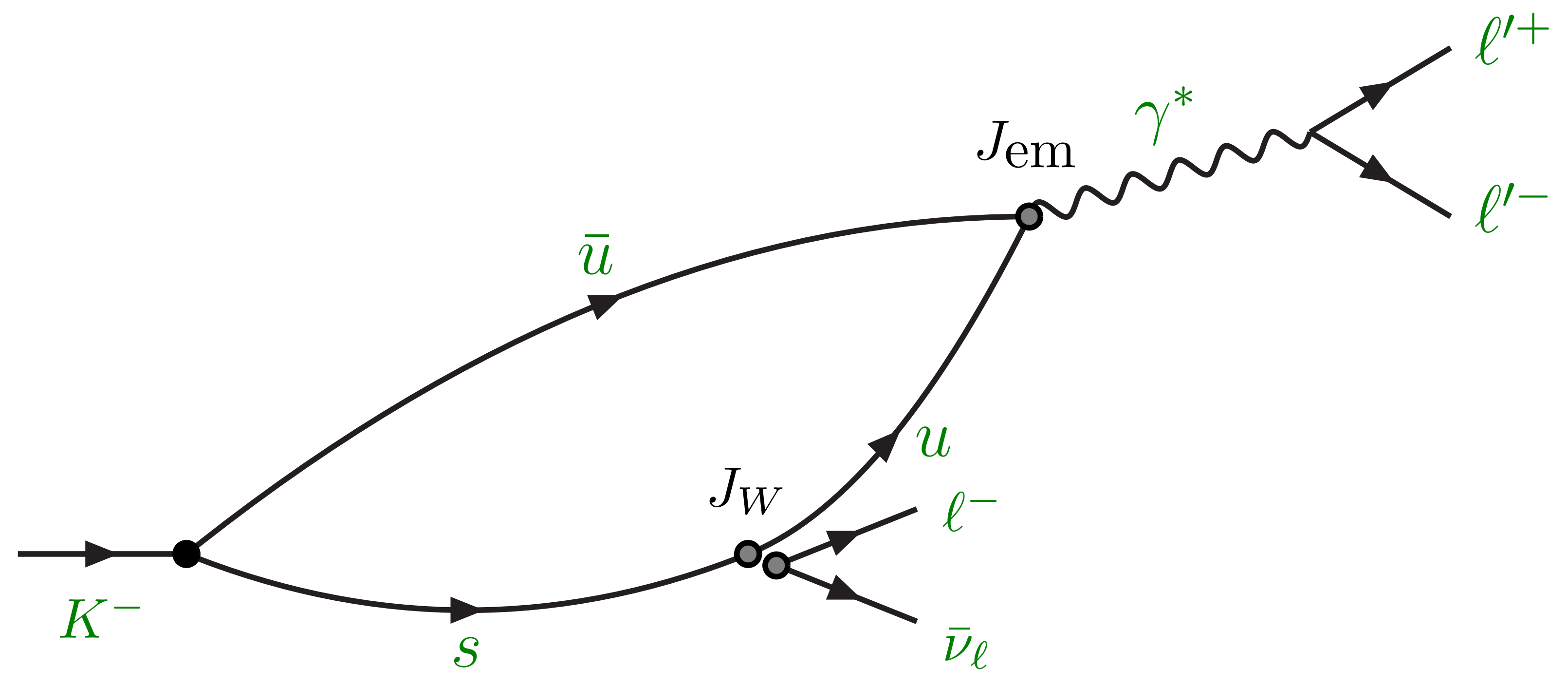


- At physical quark masses, the issue of the Minkowski → Euclidean continuation arises for sufficiently large photon virtualities.

- Frezzotti et al. have performed an exploratory and instructive study of the corresponding $D_s$ decay using the spectral density method and HLT.

R.Frezzotti et al., arXiv:2306.07228

- Computation was performed on a single ETMC ensemble, $V = 64^3 \times 128$, $a = 0.07957(13)$ fm, $m_\pi = 140.2(2)$ MeV, $m_{D_s} = 1.990(3)$ GeV.

- Necessary condition for a controlled $\epsilon \to 0$ extrapolation: $\frac{1}{L} \ll \epsilon \ll \Delta(E)$, where $\Delta(E)$ is an energy scale over which the amplitude varies significantly.

- Results below the threshold agree with the standard method.
- Difficulty arises around the sharp $\phi$ resonance where the $\epsilon \to 0$ limit cannot be taken ($\Gamma(\phi) \simeq 4.2\,\text{MeV}$ , $\epsilon \gtrsim 100\,\text{MeV}$) .
- Above the resonance there appears to be a mild dependence on $\epsilon$ .

- R. Di Palma will present first results for $K \to \ell \bar{\nu}_\ell \ell'^+ \ell'^-$ decays using the spectral density method + HLT at Latt2024.

The $\rho$-resonance is broader, making this a good channel to study (and compare with experimental results.